

1-1-2013

Assessing Corrosion Damage in Post -Tensioned Concrete Structures Using Acoustic Emission & A Preliminary Investigation Of Biopolymer Doped Cement Mortar for Use in Structural Restoration

Aditya Appalla
University of South Carolina

Follow this and additional works at: <http://scholarcommons.sc.edu/etd>

Recommended Citation

Appalla, A.(2013). *Assessing Corrosion Damage in Post -Tensioned Concrete Structures Using Acoustic Emission & A Preliminary Investigation Of Biopolymer Doped Cement Mortar for Use in Structural Restoration*. (Master's thesis). Retrieved from <http://scholarcommons.sc.edu/etd/2354>

This Open Access Thesis is brought to you for free and open access by Scholar Commons. It has been accepted for inclusion in Theses and Dissertations by an authorized administrator of Scholar Commons. For more information, please contact SCHOLARC@mailbox.sc.edu.

ASSESSING CORROSION DAMAGE IN POST-TENSIONED CONCRETE STRUCTURES
USING ACOUSTIC EMISSION & A PRELIMINARY INVESTIGATION OF BIOPOLYMER
DOPED CEMENT MORTAR FOR USE IN STRUCTURAL RESTORATION

by

Aditya Appalla

Bachelor of Technology
Bharati Vidyapeeth University, 2011

Submitted in Partial Fulfillment of the Requirements

For the Degree of Master of Science in

Civil Engineering

College of Engineering & Computing

University of South Carolina

2013

Accepted by:

Dr. Paul Ziehl, Major Professor

Dr. Navid Saleh, Committee Member

Dr. Fabio Matta, Committee Member

Dr. Juan Caicedo, Committee Member

Lacy Ford, Vice Provost and Dean of Graduate Studies

© Copyright by Aditya Appalla, 2013
All Rights Reserved.

DEDICATION

To my family!!!

ACKNOWLEDGEMENTS

This work will not be successfully completed if the efforts, inputs and support provided by people be it related to this project or in general are not acknowledged. Two years of my masters program seem to have passed really fast. This masters study is my first ever experience in a foreign country with foreign people, and I enjoyed every bit of it.

It is really hard to express my gratitude to my mentor Dr. Paul Ziehl. I consider myself lucky that I had the opportunity to work with Dr. Ziehl. During my study, I received an enormous of support from Dr Ziehl. Many – a – times I made mistakes and leant in the process, and for every time I went wrong, Dr. Ziehl was always there to correct me. A lot of what I leant here is because of Dr. Ziehl. I would also like to thank my co – advisor Dr. Navid Saleh for the time and effort he invested to complete this project.

I would like to thank all my fellow graduate students for a memorable time I had in the lab. Special thanks to Jese Mangual, William Velez, Nirupam Aich and Nima Zohadi for your valuable inputs to this project. I would like to thank Dr. Mohamed ElBatanouny for the time he spent to review my work and make recommendations to improve this project further. Mabel, Mus Kilinc, Marwa, Michael Miller, Mozahid, Tyler Davis and Frank Taylor thank you all. Finally I would like to express my gratitude to my family for their unconditional love and support.

ABSTRACT

A sizeable portion of the civil infrastructure is made from concrete. An estimate shows that about 7 billion cubic meters of concrete is made annually worldwide. With the deterioration of the infrastructure due to aging or external factors, significant monetary and technological investment is needed for condition evaluation, maintenance and repair. Two areas that account for a considerable portion of this investment are condition evaluation for maintenance of corroded concrete structures and mortar patching for repair and rehabilitation.

The primary method of evaluation of a structure is by visual inspection. But this method is limited as some crucial areas in a structure are either completely inaccessible or very difficult to access. Monitoring corrosion in the prestressing strands of post-tensioned [PT] concrete structures is one such example. In post-tensioned concrete structures, the prestressing reinforcement is located deep within the structure and is difficult to access. The reinforcement in these structures when exposed to chlorides starts to corrode and the inaccessibility of the prestressing reinforcement makes condition evaluation much more difficult. Under such circumstances a structural health monitoring [SHM] method is needed to aid in the condition evaluation. Acoustic emission [AE] is one such SHM method that has the ability to evaluate the structure to improve maintenance procedures on post-tensioned concrete structures.

In the first part of the thesis, long term corrosion monitoring studies were performed on specimens representing internal and external post-tensioned methods of

construction of concrete structures. Corrosion was induced by adding additional chlorides in the grout mix or by performing wet-dry cycling of NaCl solution. The corrosion process in each specimen was monitored by two acoustic emission R6i sensors and an embedded silver chloride reference electrode for half cell potential [HCP] measurements. Appropriate filters were developed to minimize noise in the AE data and the filtered AE data was validated by HCP measurements. Results also indicate that intensity analysis is a very helpful technique in quantifying the degree of damage in the specimens.

In the second part of this thesis, studies are focused on repair and rehabilitation. The majority of the small to medium scale repair work in concrete structures is done by patch working that uses regular cement mortar doped with additives. These additives help to enhance the properties of regular mortar such as strength, durability, shrinkage, and curing time. Some examples of such additives are ground granulated blast furnace slag [GGBS], silica fume, magnesium, fly ash, or other polymeric additives such as styrene butadiene, polyvinyl acetate, and acrylics. Cement in the mortar is replaced with these additives by about 10 – 20% by weight to achieve enhanced properties, making the patch works expensive.

Dopamine hydrochloride, commonly known as dopamine, is a non-toxic organic biopolymer that has shown promise as a polymeric additive for patch repair work. A preliminary investigation was performed on dopamine doped cement mortars for patch repair work. To evaluate the effect of dopamine on properties of cement mortar, two inch cubes were cast and tested in compression. One of the biggest advantages of dopamine is that while most polymeric additives replace cement by 10 – 20%, dopamine is required only in very minute quantities of 0.05% weight of cement making the patch work very

inexpensive. Results also indicate that dopamine is able to enhance the strength, load-deformation behavior and curing time of regular cement mortar.

TABLE OF CONTENTS

DEDICATION	iii
ACKNOWLEDGEMENTS.....	iv
ABSTRACT	v
LIST OF TABLES	x
LIST OF FIGURES	xi
LIST OF ABBREVIATIONS.....	xi
CHAPTER – 1: INTRODUCTION	1
1.1. INTRODUCTION TO PRESTRESSING TECHNOLOGY	1
1.2. OVERVIEW OF ACOUSTIC EMISSION MONITORING.....	10
1.3. LAYOUT OF THESIS.....	14
REFERENCES.....	15
CHAPTER – 2	17
ASSESSING CORROSION DAMAGE IN POST-TENSIONED CONCRETE STRUCTURES USING ACOUSTIC EMISSION ¹	17
2.1. ABSTRACT.....	18
2.2. INTRODUCTION.....	19
2.3. RESEARCH SIGNIFICANCE	22
2.4. LITERATURE REVIEW.....	22
2.5. EXPERIMENTAL SETUP	25
2.6. RESULTS AND DISCUSSIONS	29
2.7. CONCLUSIONS.....	35
REFERENCES.....	36

CHAPTER – 3	53
A PRELIMINARY INVESTIGATION OF BIOPOLYMER DOPED CEMENT MORTARS FOR USE IN STRUCTURAL RESTORATION ¹	53
3.1. ABSTRACT	54
3.2. INTRODUCTION.....	55
3.3. MATERIALS AND PREPARATION.....	57
3.4. EXPERIMENTAL PROCEDURE	57
3.5. TEST RESULTS	58
3.6. SEM IMAGING RESULTS	59
3.7. CONCLUSIONS.....	59
REFERENCES.....	61
BIBLIOGRAPHY	68

LIST OF TABLES

Table 1.1: Advantages & Disadvantages of Internal and External PT	3
Table 2. 1: Concrete mix design for internal PT specimens.	40
Table 2. 2: AE waveform filters	40
Table 2. 3: ASTM corrosion for AgCl reference electrode (Broomfield, 2007)	41
Table 3.1: Seven days compressive strength for dopamine mortar specimens.....	63
Table 3.2: Seven days compressive strength for control mortar specimens	63
Table 3.3: Twenty eight days compressive strength for dopamine mortar specimens	63
Table 3.4: Twenty eight days strength for control mortar specimens.....	64

LIST OF FIGURES

Figure 1.1: External Post-Tensioning in a bridge (www.cclint.com)	4
Figure 1.2: Internal Bonded PT (www.lowryavenuebridge.com)	4
Figure 1.3: Corroded anchorage in Mid Bay Bridge (www.dot.state.oh.us)	7
Figure 1.4: Cracked duct showing severely corroded strand (www.dot.state.oh.us).....	8
Figure 1.5: Slipping of duct at deviator block (www.dot.state.oh.us)	8
Figure 1.6: Boroscope photo of tendon in Mid Bay Bridge (www.dot.state.oh.us)	9
Figure 1. 7: Lowes Motor Speedway Bridge Collapse, May 2000, US (www.onlineathens.com)	10
Figure 1.8: AE Source Mechanism.....	11
Figure 2. 1: General experimental layout for PT specimens	41
Figure 2. 2: External Post-Tensioned Specimens: (a) Control, E1; (b) Wet-dry 4 ft, E2; (c) Exposed Strand, E3; and (d) Wet-dry 10ft, E4	42
Figure 2. 3: Top view of specimen E3	43
Figure 2. 4: Groove to facilitate wet-dry cycles	43
Figure 2. 5: Internal PT Specimens: (a) 0.08% Cl, I1; (b) 0.8% Cl, I2; (c) 1.6% Cl, 4ft, I3; and (d) 1.6% Cl, 10ft, I4	44
Figure 2. 6: R6i AE sensor (Mistras Group, Inc.)	44
Figure 2. 7: Positioning of sensors on internal PT specimens.....	45
Figure 2. 8: Positioning of sensors on external PT specimens	45
Figure 2. 9: CSS vs. time and HCP vs. time for external PT specimens.....	46

Figure 2. 10: Amplitude vs. time for specimens a) E2, b) E4 illustrating corrosion in dry cycling	47
Figure 2. 11: Visible corrosion in specimen E3	47
Figure 2. 12: Duration vs. Amplitude for external PT specimens	48
Figure 2. 13: Amplitude vs. time for external PT specimens	49
Figure 2. 14: CSS vs. time and HCP vs. time for internal PT specimens.....	50
Figure 2. 15: Duration vs. Amplitude for internal PT specimens.....	50
Figure 2. 16: Amplitude vs. time for internal PT specimens.....	51
Figure 2. 17: Intensity analysis chart for external PT specimens	51
Figure 2. 18: Intensity analysis chart for internal PT specimens.....	52
Figure 2. 19: Source location for (a) specimen E2 (b) specimen E3	52
Figure 3.1: Seven days load vs. deflection curves for dopamine mortar specimen.....	64
Figure 3.2: Twenty eight days load vs. deflection curves for dopamine mortar specimens.....	65
Figure 3.3: Seven days load vs. deflection curves for control specimens	65
Figure 3.4: Twenty eight days load vs. deflection curves for control specimens.....	66
Figure 3. 5: Scanning electron micrographs of (a) control, (b) biopolymer added concrete at 7 days, and (c) biopolymer added concrete at 28 days.	67

LIST OF ABBREVIATIONS

PT	Post-Tensioning
HDPE	High Density Poly Ethylene
PP	Poly Propylene
AE	Acoustic Emission
HCP	Half Cell Potential
CSS	Cumulative Signal Strength
RMS	Root Mean Square

CHAPTER – 1: INTRODUCTION

This chapter is divided into three main sections. The first section is an introduction to construction of concrete structures using prestressing technology followed by a few examples of corrosion in post-tensioned concrete structures. The second section is a brief overview of some basic concepts and terminology related to Acoustic Emission. The final section details the layout and the objectives of the work done in this thesis.

1.1. INTRODUCTION TO PRESTRESSING TECHNOLOGY

Concrete is a brittle material with compressive strength values far exceeding those for tensile strength. Prestressing is a method of construction of concrete structures where internal tensile stress is applied so that the concrete remains in compression when external loads are applied. One of the earliest examples of prestressing is the construction of wooden barrels by force fitting of metal bands. In 1904 Eugene Freyssinet pioneered the method of prestressing which has now become a major construction practice for concrete structures.

Prestressed concrete offers many advantages in comparison to passively reinforced concrete structures. Some advantages of prestressed structural members are a) the concrete is either free from tensile stress or very low tensile stress is allowed; b) the uncracked moment of inertia can be utilized, thus saving on material costs; c) improved resistance to shear due to the imposed compressive stress; and d) reduced on-site construction time. The use of high strength concrete and steel results in lighter member cross-sections and therefore reduced dead loads. These features also contribute to improved durability of the structure under aggressive environmental conditions. Standardized prestressed bridge girders between 9.5 m (30 ft) and 27.5 m (90 ft) are significantly more economical than steel or reinforced concrete girders, and the trend is to utilize prestressed for girders of spans up to 46 m (150 ft).

Prestressing is subdivided into two categories; Pretensioning and Post-Tensioning [PT]. In pretensioning, the tendons are laid first and stressed after which the concrete is placed. In post-tensioning [PT], tendons are laid in ducts and are stressed after concrete has been placed and hardened. Post-tensioning [PT] can be further divided into internal and external post-tensioning. In external post-tensioning [PT], the strands are laid outside the structure, whereas for internal post-tensioning the ducts pass within the structure and are covered by the concrete.

For internal post-tensioning [PT], the ducts can be grouted which are known as bonded post-tensioning [PT] or in some cases not grouted, also known as unbonded post-tensioning. Bonded post-tensioned ducts are generally 2.5 times the diameter of the strand and generally carry multiple strands. On the other hand unbonded post-tensioned ducts are the size of the strand and have the provision to carry only a single stand. In

unbonded post-tensioning, the strands are greased before passing them into ducts and tensioning. For an example, unbonded post-tensioning has its applications in slabs where the thickness of the slab is not sufficient to accommodate a bigger duct, while bonded post-tensioning is use in case of large scale structures like bridge girders or decks. Since the 1960's, post-tensioning [PT] (internal and external PT) has become a popular and accepted method for construction for bridges across the United States and throughout out the world. Ease of construction, higher strengths, and low costs have contributed to this popularity.

Each of the methods of post-tensioning has advantages and disadvantages, as listed in Table 1.1.

Table 1.1: Advantages & Disadvantages of Internal and External PT

Internal Post-Tensioning	
Advantages	Disadvantages
<ol style="list-style-type: none"> 1. Less prone to damage. 2. Strands are laid as per the bending moment diagram; hence the loads are properly balanced. 	<ol style="list-style-type: none"> 1. Rigorous maintenance and repair procedures. Some locations are completely inaccessible.
External Post-Tensioning	
Advantages	Disadvantages
<ol style="list-style-type: none"> 1. Smaller sections required so reduced dead weight. 2. Reduced material, therefore lower costs. 3. Reduced maintenance and repair. 	<ol style="list-style-type: none"> 1. More prone to damage because the strands are located outside the structure.

Both of these methods of PT were developed at the same time, and are extensively used. In some cases like bridges, mixed post-tensioning is also preferred wherein both internal and external post-tensioning is adopted. In both external and internal PT, the tendons pass through either metal, High Density Poly Ethylene [HDPE], or poly propylene ducts to transfer stresses from the strands to the concrete. Figure 1.1 and 1.2 shows external and internal post-tensioning.



Figure 1.1: External Post-Tensioning in a bridge (www.cclint.com)

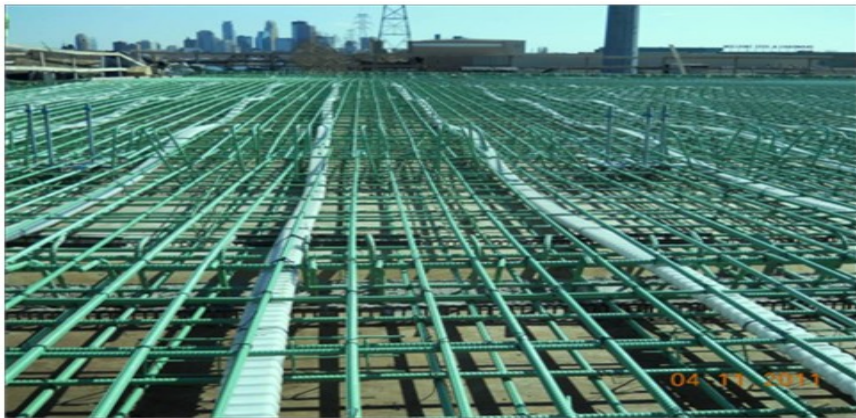


Figure 1.2: Internal Bonded PT (www.lowryavenuebridge.com)

1.1.1. Basic Prestressing Terminology

Some of the basic terminology related to prestressing is provided below for convenience:

Strand – A high tensile cable made of steel, typically comprised of seven individual wires, with six wires helically wound around a single central wire. Strands for post-tensioning purpose are typically Grade 1,860 MPa (270 ksi) conforming to ASTM A416 [1]. It is commonly available in two sizes, 12.7 mm (0.5 in) and 15.24 mm (0.6 in) diameter. These strands are manufactured by a cold drawing process which makes them resistant to corrosion.

Tendons – A group of strands that are connected to the same anchor and located in the same duct is known as a tendon. A typical post-tensioned bridge segment has many groups of tendons laid in various positions.

Ducts – Hollow structures made either from High Density Poly Ethylene [HDPE] or metal, through which tendons pass. Ducts can be laid within or outside the structure. The external surface can be corrugated or smooth depending on where the ducts are being laid. For internal post-tensioning, corrugated ducts are used as they provide improved bond strength. The diameter of the ducts is generally 2.5 times the diameter of the tendons.

Grout – A mix of cement, fine aggregates, and admixtures in a certain proportion which meets the requirements of ASTM C953, ASTM C942, ASTM C1202, ASTM C1090, ASTM C939, and/or ASTM C940. Water cement ratio is generally limited to 0.45 to minimize bleeding. These grouts can be mixed in the field per an approved design or can be pre-bagged by a manufacturer.

Void – A void is an internal air pocket in the grouted ducts. Voids occur due to improper grouting practices or bleeding. They trap moisture and can lead to corrosion of the tendon or strand.

Anchorage – A device used to enable the tendon to impart and maintain the desired range of stress in the concrete.

Pretensioning – A method of prestressing in which the tendons are tensioned before the concrete is placed.

Post-tensioning – A method of prestressing wherein the strands are stressed after hardening of the concrete.

Full Prestressing – Prestressed concrete in which tensile stresses in the concrete are entirely negated at working loads by having sufficiently high prestress in the member.

Partial Prestressing –The degree of prestress applied to concrete in which tensile stresses to a limited magnitude are permitted in concrete under working loads.

1.1.2. Corrosion in Post-Tensioned Bridges

Initially it was believed that post-tensioning was a low maintenance method of construction. However, the sudden failure of the Bickton Meadows foot bridge in 1967 and the Ynys-y-Gwas bridge in 1985 raised questions about the durability of this construction method.

Of 600,000 bridges in the U.S., roughly 18% are prestressed. Some of these are exhibiting corrosion in the prestressing strands. Major factors for corrosion include carbonation, high chlorides in the grout mix, ingress of chlorides due to the environment (deicing salts or location of the bridge in coastal regions), air pockets in ducts, bleed water, and faulty construction practices. High corrosion levels have been found in Florida due to the coastal climate. Some of the major bridges in that area include the Sunshine Skyway Bridge, the Niles Channel Bridge, and the Mid Bay Bridge. The Mid Bay Bridge was opened in 1993, and by 2000 the corrosion levels in some tendons were so high that 11 tendons in the bridge had to be replaced. The same was observed in the Skyway Bridge and the Niles channel bridge. Figure 1.3 shows severe corrosion in the anchorages of Mid Bay Bridge.



Figure 1.3: Corroded anchorage in Mid Bay Bridge (www.dot.state.oh.us)

It was also observed that cracking of the ducts due to faulty construction practices or slipping of the ducts at deviator blocks or anchorages in the Mid Bay Bridge left the strand exposed to the environment, thereby accelerating the corrosion process. In Figure 1.4 and 1.5 show cracking and slipping of ducts in the Mid Bay Bridge.



Figure 1.4: Cracked duct showing severely corroded strand (www.dot.state.oh.us)



Figure 1.5: Slipping of duct at deviator block (www.dot.state.oh.us)

Further boroscopic inspections revealed corrosion in many other tendons. Figure 1.6 shows a boroscope photograph of a corroded strand in the Mid Bay Bridge.

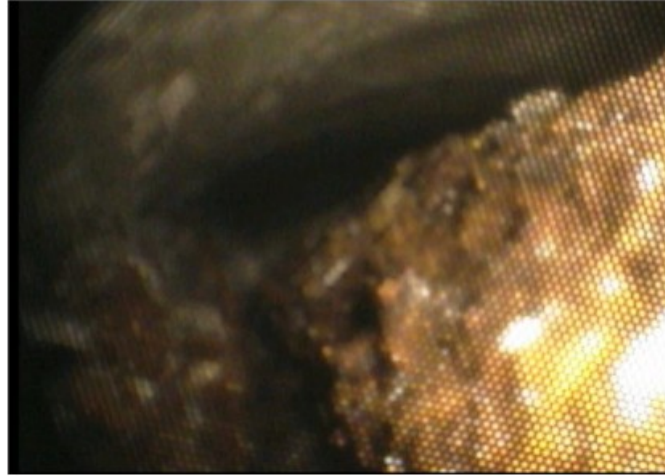


Figure 1.6: Boroscope photo of tendon in Mid Bay Bridge (www.dot.state.oh.us)

In May 2000, a 24.5 m (80-ft) section of the Lowes Motor Speedway Bridge in North Carolina collapsed killing and injuring several people. Investigations have revealed that the cause of the collapse was corrosion of the strands. This was in turn due to the use of a grout with excess calcium chloride during the general repair and maintenance procedures of the bridge. Figure 1.7 shows the collapsed section of the Lowes Motor Speedway Bridge. In 2011, the FHWA released a list of 35 post-tensioned bridges across the U.S. that are experiencing corrosion in their strands due to excess chlorides in the grout mix, and the list is expected to increase.



Figure 1. 7: Lowe's Motor Speedway Bridge Collapse, May 2000, US
(www.onlineathens.com)

1.2. OVERVIEW OF ACOUSTIC EMISSION MONITORING

As per ASTM E1316, Acoustic Emission [AE] is defined as ‘*the class of phenomenon whereby transient elastic waves are generated by rapid release of energy from localized sources within a material, or the transient waves so generated*’.

When a material is stressed, cracked or deformed, the internal particles realign themselves and release energy in the form of stress waves. These stress waves can be detected by piezoelectric sensors which convert this energy into electrical signals. Each signal has properties that can be analyzed.

Some of detectable sources are crack growth, dislocations, corrosion, friction, leaks, and cavitations. Some advantages of AE include:

- a. The energy detected comes from within the material itself.

- b. It has the capability of providing real time structural health monitoring and damage locations can be identified.

However one of the interesting aspects of AE monitoring is that existing defects cannot be detected unless they are actively releasing energy. Therefore, if a crack or other defect is not growing (for example a crack that is self-arresting), AE activity will not be detected from that crack unless other sources are present, such as friction (also referred to as fretting). A schematic of AE mechanism is shown in Figure 1.8.

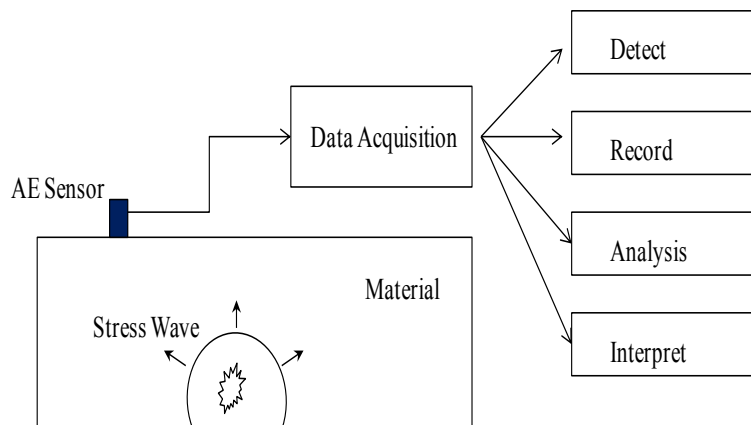


Figure 1.8: AE Source Mechanism

1.2.1. Typical Parameters of Acoustic Emission

The basic parameters of an AE signal are discussed in this section. To obtain a better understanding of the process occurring in a material, these AE parameters must be studied in combination to draw proper conclusions. ASTM E1316 is referenced for the definitions of AE parameters. Some of the AE parameters are defined below:

Hit – It is defined as the detection and measurement of an AE signal on and individual sensor channel.

Event – A local material change that gives rise to an acoustic emission. A single event can result in a number of hits.

Voltage Threshold – The voltage level on an electronic comparator such that signals with amplitudes larger than this level will be recognized. The threshold can be user defined or automatic floating. This is an important feature that helps to minimize noise.

Amplitude – It is defined as the magnitude of a peak voltage of the largest excursion attained by the signal waveform from a single emission event. Amplitude is measured in decibels (dB). Amplitude is obtained from the signal voltage by the below mentioned equation:

$$A = 20 \log \frac{V}{V_{ref}} \quad (\text{Eq.1})$$

where,

V – Voltage of peak signal

V_{ref} – Reference voltage, dependent on the type of sensor

Duration – Defined as the time between AE signal start and AE signal stop. In other words it is the time from the first threshold crossing to the last threshold crossing and is usually measured in micro seconds (μs).

Rise Time – It is defined as the time between AE signal start and peak amplitude of that signal and is measured in micro seconds (μs).

Signal Strength – It is defined as the measured area of the rectified AE signal with units measured in volt-sec. The formula for signal strength is given in Equation 2.

$$S = \frac{1}{2} [\int_{t_1}^{t_2} f_+ (t). dt + \int_{t_1}^{t_2} f_- (t). dt] \quad (\text{Eq.2})$$

Where, S is signal strength, f_+ and f_- is positive and negative signal function.

Signal Energy – It is the energy contained in an acoustic emission burst signal, and is usually measured in joules.

Count – It is the number of times the acoustic emission signal exceeds a preset threshold during any selected portion of the test, and count rate is the number of counts during a fixed period of time.

Frequency – The number of cycles per second of an AE signal is known as its frequency, typically with units of kHz. Frequency is not a constant value for any hit. Commonly the average frequency is reported.

Root Mean Square (RMS) – Defined as the rectified time averaged AE signal, measured on a linear scale and reported in volts. RMS is the measure of continuously varying AE signal voltage.

The above recorded parameters of AE can be filtered for noise removal and analyzed using some of the damage quantification methods mentioned below:

- a. Intensity Analysis
- b. Felicity and Kaiser Effect
- c. Calm ratio vs. load ratio

- d. Peak Cumulative Signal Strength Ratio
- e. Relaxation Ratio
- f. b-value and Ib-value

1.3. LAYOUT OF THESIS

This thesis is divided into three chapters. Chapter 2 discusses the investigation carried out on the potential applicability of Acoustic Emission in real time to detect corrosion in post-tensioned concrete structures. Corrosion levels were monitored using half-cell potentials and acoustic emission on a total of eight specimens that were representative of internal and external pos-tensioning methods of construction. Objective of the study was to a) monitor corrosion process using acoustic emission in specimens that are similar to a realistic setting b) quantify corrosion damage in the specimens c) develop filters that can used to effectively minimize noise in acoustic emission data d) quantify the damage in specimens due to corrosion using intensity analysis technique.

Chapter 3 discusses the application of dopamine into cement mortar for patch working. Two inch cement mortar cubes doped with 0.5% dopamine by weight of cement were cast and tested in compression. The objective of the study was to a) show that dopamine can be incorporated for use in structural repair b) study the change in the affects in properties of regular cement mortar when doped with dopamine c) prove that only a minute quantities of dopamine is required to achieve desired results in cement mortars.

REFERENCES

1. FHWA – Post Tensioning Tendon Installation And Grouting Manual, 2004
2. Durability And Sustainability of Concrete Bridges, FDOT & PCI Presentation, 2009
3. Evaluation of External Post Tensioned Tendons Using Vibration Signatures, Dissertation, Jun Ki Lee, 2007
4. Electrochemical Characterization and Time Variant Structural Reliability Assessment of Post – Tensioned Segmental Concrete Bridges, Dissertation, Radhakrishna.G. Pillai, 2009.
5. Prestressed Concrete, Edward Nawy, Fifth Edition
6. Podolny, Walter Jr., 1992, "Corrosion of prestressing steels and its mitigation", PCI Journal, Volume: 37, Issue: 5.
7. Woodward, R.J. and William, F.W., 1988, "Collapse of Ynys – y – Gwas Bridge, West Glamorgan," Proceedings of Institute of Civil Engineers, Part 1, Volume.84, pp.635-669.
8. Florida Department of Transportation, 2001a, "Mid bay Bridge Post – Tensioning Evaluation," Final Report, Corven Engineering, Inc., FDOT, Tallahassee, FL, 2622pp.
9. Florida Department of Transportation, 2001b, "Sunshine Skyway Bridge Post – Tensioned tendons Investigation," Parsons Brinckerhoff Quade and Douglas, Inc., FDOT, Tallahassee, FL.
10. Federal Highway Administration (FHWA), 2011, "Elevated Chloride Levels in Sika Grout 300 PT Cementitious Grout", Memorandum.

11. Xu, J. (2008). “Nondestructive evaluation of prestressed concrete structures by means of acoustic emission monitoring”, Dissertation, Dept. of Civil Engineering, Univ. of Auburn, Auburn, Alabama.
12. Dickson. T.J., Tabatabai. H., Whiting. D.A., “Corrosion Assesment of a 34 Year Old Precast Post – tensioned Concrete Girder”, PCI Journal, Nov – Dec 1993.
13. Hamilton. H.R., Wheat. H.G., Breen. J.E., Frank. K.H., “Corrosion testing of Grout for Post-tensioning Ducts and Stay Cables”, Journal of Structural Engineering, Feb 2000.
14. West. J.S., Breen. J.E., Vignos. R.P., “Evaluation of Corrosion Protection for Internal Prestressing Tendons in Precast segmental bridges”, PCI Journal.
15. Salas. R.M., Schokker. A.J, West. J.S., Breen. J.E., Kreger. M.E., “Corrosion Risk of Bonded Post Tensioned Concrete Elements”, PCI Journal, Jan – Feb 2008.
16. Mangual, J., ElBatanouny, M. K., Ziehl, P., and Matta, F. (2013). “Acoustic-Emission-Based Characterization of Corrosion Damage in Cracked Concrete with Prestressing Strand”. ACI Materials Journal, 110(1), 89.
17. Mangual, J., ElBatanouny, M., Ziehl, P., and Matta, F., “Corrosion Damage Quantification of Prestressing Strands Using Acoustic Emission”, ASCE Journal of Materials in Civil Engineering, in press, August 2012.

CHAPTER – 2

ASSESSING CORROSION DAMAGE IN POST-TENSIONED CONCRETE STRUCTURES USING ACOUSTIC EMISSION¹

¹Aditya Appalla, Mohamed ElBatanouny, William Velez, Paul Ziehl, To be submitted to ASCE Journal of Materials in Civil Engineering.

2.1. ABSTRACT

The ingress of chlorides into Post-Tensioned [PT] concrete structures is a leading cause of corrosion of the prestressing strands. This reduces the strength, durability, and service life and may even result in catastrophic failure. A Structural Health Monitoring [SHM] method is needed to improve the maintenance procedures of these structures. To evaluate the potential of acoustic emission monitoring for this application, long term corrosion monitoring tests were performed on specimens that were representative of internal and external post-tensioning methods of construction. Corrosion was induced in the specimens by adding chlorides or by performing wet-dry cycling with NaCl solution. The corrosion process was monitored by half cell potential measurements [HCP] and acoustic emission [AE]. Results show that AE has the ability to detect and quantify corrosion initiation, propagation, and cracking in the PT specimens with the same accuracy as HCP measurements. Further intensity analysis of AE data shows that the damage in the PT specimens can be categorized according to the levels of corrosion present. This investigation demonstrates that AE can be successfully implemented to detect, monitor, and quantify corrosion levels in PT concrete structures, and that AE is a promising SHM and assessment method to detect corrosion in the absence of regular electrochemical techniques.

Keywords: Post-Tensioned, Concrete, Corrosion, Steel, Acoustic Emission, Half Cell Potentials

2.2. INTRODUCTION

The method of construction of concrete structures where highly stressed strands passing through high density polyethylene [HDPE] or poly propylene [PP] ducts in a concrete structure to transfer the stresses from the strands to concrete is known as Post-Tensioning [PT]. Some of the advantages of post-tensioned structures are higher strength, smaller cross-sections, low or no cracking, ease of construction, and related economic viability. Post-Tensioned structures are either bonded or unbonded. In bonded post-tensioning, the strands are passed through ducts that are later filled with a cement based grout whereas the ducts of unbonded post-tensioned structures are left ungrouted. Bonded post-tensioning ducts are generally 2.5 times the diameter of the tendon and are used in structures with bigger cross-sections, while unbonded post-tensioned ducts have the provision to pass only a single strand, and are used in structures with smaller cross-section where there is a limitation for using bigger size ducts. Further in this paper only bonded post-tensioning is discussed.

Post-tensioned structures are categorized into two types; external and internal. In external post-tensioning, the strands are covered in grouted ducts that are laid outside the concrete structure, whereas internally post-tensioned structures have strands in grouted ducts placed within the concrete itself.

Several bridges constructed using post-tensioning are experiencing damage in their strands due to corrosion [1-9]. Corrosion of the strands is an irreversible process that compromises the strength, safety, and serviceability of the bridge. Further the corrosion by-products are expansive in nature and cause cracking of grout or concrete around the

strand. The high alkalinity of the cement grout, with pH values generally ranging between 12 and 13, serves to protect the strands from corrosion by forming a microscopic layer of oxide over the surface of the reinforcement which is known as passivation. This passivating layer of oxide may be broken down by the ingress of chlorides into the ducts due to deicing salts, faulty construction practice, or location of bridges near coastal areas.

In some cases, unusually high levels of chlorides have been observed in the grout itself that is used for post-tensioning purposes due to improper manufacturing processes [10]. The chloride levels detected in some post-tensioned structures have exceeded the maximum permissible chloride limit of 0.08% by weight of cement material as prescribed by FHWA to a very high percentage. A very recent example is the Sika 300 PT grout which was used by many state Departments of Transportation across the U.S. High chloride levels were observed in this grout, which were up to 400% (four times) the maximum permissible limit causing deterioration of the prestressing strands in the bridges for which it was used. The existence of air voids in the ducts due to bleed water and carbonation are other major causes for corrosion of the prestressing strands.

External PT structures may be likely to corrode faster due to exposure to the environment, and the corrosion process is mostly due to deicing salts or harsh environment. Internal PT structures are less susceptible to corrosion due to atmospheric conditions as the strands are encased in the duct which is covered with a thick layer of concrete. However, the presence of chlorides in the grout mix initiates corrosion of the strands in internal PT structures and its detection and repair is difficult due to the concrete cover. On the other hand detecting corrosion in external PT systems is more readily accomplished. Visual inspection of post-tensioned bridges is difficult and they

often lack a provision for electrochemical measurements to determine the corrosion levels in prestressing strands. As such, a structural health monitoring [SHM] method is needed to evaluate the damage in the prestressing strands. Acoustic Emission [AE] is one such method that may offer a solution. Research has shown that AE can be effectively used to detect corrosion in concrete structures [11-21].

Previous research has largely focused on the use of AE to detect corrosion of passive reinforcement, and some studies have focused on prestressing applications. This paper investigates the use of AE to detect corrosion in active prestressing strands in a setting that is representative of both internal and external bonded post-tensioning.

Eight specimens (including two control specimens) were fabricated; four internal and four external PT. Wet-dry cycling was performed on the external PT specimens and additional chlorides were added to the internal PT specimens. Corrosion in each specimen was monitored with two AE sensors and an embedded silver chloride reference electrode. The AE data was validated by electrochemical measurements such as half cell potentials [HCP]. HCP measurements were taken on a weekly basis and AE activity was continuously recorded for four months. Raw AE data was filtered and correlated to HCP measurements to investigate the ability of AE to monitor and assess the state of corrosion damage.

2.3. RESEARCH SIGNIFICANCE

Corrosion of prestressing strands in post-tensioned structures is a slow process. However this process is accelerated due to ingress of chlorides or excess chlorides in the grout mix, resulting in reduced strength and service life, higher maintenance costs or even potential failure of the structure. Acoustic Emission [AE] is a Structural Health Monitoring [SHM] method that can be employed to investigate corrosion in post-tensioned bridges. This paper investigates the implementation of AE for the detection of corrosion in bridges constructed using both internal and external methods of post-tensioning.

2.4. LITERATURE REVIEW

Idrisi et al. (2003) [22] investigated corrosion in steel reinforcement of diameter 5 mm (1/5 in.) centrally inserted to a depth of 60 mm (2-1/3 in.) into mortar specimens of diameter 30 mm (1-1/5 in.) and length 90 mm (3- 1/2 in.). The mortar specimens were made with two different w/c ratios of 0.5 and 0.75. The specimens were then allowed to cure to minimize AE due to shrinkage. The top surfaces of the specimens were polished with sand paper to attach R15 AE sensors. A platinum mesh acted as a counter electrode and a saturated calomel electrode acted as a reference electrode. Corrosion was induced in the specimens by immersing the specimens into a 6% NaCl solution.

The initial pH of the specimens was 11.5 which is sufficient to create a passive layer. Upon alternating immersion of the sample every 24 hrs, the pH gradually reduced to 8 breaking the passive later and inducing corrosion. It was also observed that the

corrosion behavior of the reinforcement was different with different water/cement ratio. Higher water/cement ratio mixes had higher porosity and therefore more corrosion.

The AE activity for the specimen with $w/c = 0.75$ started very quickly after immersion into solution and was characterized by stronger AE signals. Specimens with $w/c = 0.5$ had weaker AE signals with duration and rise time less than $20 \mu s$. This shows that porosity is dependent on w/c ratio and affects the corrosion and AE activity. The authors also concluded that there is a correlation between AE activity and corrosion density.

Ohtsu et al. (2008) [23] performed accelerated corrosion tests and wet-dry cycling of 3% NaCl solution on reinforced concrete specimens of size 400 mm x 250 mm x 100 mm ($15 \frac{3}{4} \times 10 \times 4$ in.). The specimens were placed in an open top container on a copper plate that acted as the cathode and the reinforcement in the specimen acted as the anode. Wet-dry cycling was performed on a weekly basis with specimens in the solution for one week and then kept dry for the next week. A current of 100 mA was constantly supplied between the reinforcing steel and copper plate. Each specimen had two AE sensors, and a copper sulphate reference electrode was used for the half-cell potential measurements.

A plot of RA and average frequency was employed to analyze the AE data, with RA values plotted on the x – axis and average frequency on the y – axis. RA is the ratio of rise time to maximum amplitude and average frequency is the average of the frequencies in kHz over the entire AE hit. High AE activity was recorded at 40 days and 100 days. At 40 days the RA value was very high and average frequency was very low.

These were classified as shear cracks. The authors state that high average frequency and low RA are indicative of tensile cracking, and this was observed at 100 days. The authors also state that corrosion cracks are classified as tensile cracks. A final conclusion is that the initial cracks were shear cracks and mark corrosion initiation, and the larger cracks at later stages were tensile cracks due to corrosion byproducts and concrete cracking.

Ramadan et al. (2008) [24] carried out tests on 12.5 mm (1/2 in.) diameter seven wire prestressing strand that was stressed to 80% of its ultimate capacity. Four wide band WD acoustic emission sensors were directly attached to the strand to record AE activity with a 23 dB test threshold. To accelerate corrosion of the strand, an electrochemical cell with concrete pore solution surrounded the strand. A saturated calomel electrode was used as the reference electrode and a platinum disk as the counter electrode.

The time to failure of the wire was approximately 34 days. The plot of cumulative hits versus time was divided into three stages. The first stage is cracking due to local corrosion, the second stage is crack growth and propagation, and the third stage is failure of the wire. The amplitudes ranged between 23 and 30 dB in the first stage and 30 and 40 dB in the second stage. Pitting corrosion was characterized by peak frequency of 140 kHz, and corrosion propagation was characterized by peak frequency of 200 kHz. Wire failure was attributed to amplitudes greater than 55 dB. In SEM images, severe pitting corrosion was reported with hydrogen entrapped in the matrix.

In summary, the majority of the literature focuses on using passive prestressing steel reinforcement, with the exception of Ramadan, 2008. Accelerated corrosion processes and concrete pore solution were adopted to achieve desired levels of corrosion.

In real time the corrosion rate is very slow and the factors affecting corrosion are mainly chlorides and carbonation. Secondly there is always a hindrance to AE signals due to thick concrete cover and the plastic ducts. Appropriate filters for AE need to be developed to minimize noise and retain corrosion data in realistic applications. Very little literature has been reported for detecting corrosion in post-tensioned concrete structure with acoustic emission. This investigation was designed keeping in view the limitations of previous research and to enable an assessment of the applicability of AE in a realistic setting.

2.5. EXPERIMENTAL SETUP

The experimental setup was designed to be representative of both external and internal PT systems. Two 12.5 mm ($\frac{1}{2}$ in.) diameter seven wire strands of length 19.5 m (58 ft.) were stressed and supported on two steel reaction frames. A total of eight specimens were created around the strands, of which four specimens represent external PT and the remaining four represent internal PT. Anchor blocks made of concrete were cast around the strands and in-between specimens for safety in the event of strand failure due to corrosion. Figure 2.1 is a schematic of the experiential setup.

2.5.1. Externally Post-Tensioned Specimens

Four external PT specimens were created by encasing a seven wire 12.5 mm ($\frac{1}{2}$ in.) diameter low relaxation strand in a HDPE duct of smooth external surface with a

diameter of 60.3 mm (2-3/8 in) and thickness of 6 mm (1/4 in.). Figures 2.2 (a-d) represent the external post-tensioned specimens. The strand was stressed to $0.7f_{pu}$ (guaranteed ultimate strength, $f_{pu} = 270$ ksi) through the application of an axial tensile force. A cement based grout manufactured by BASF (BASF Masterflow 1205) was used for grouting. This grout is a special grout specifically for PT structures and is also used by many DOT's across the U.S. A water quantity of 1,100 ml was added for every 4.54 kg (10 lbs.) of grout. This mix provides good consistency and fluidity for pumping into ducts. For these specimens no additional chlorides were added to the grout mix. Of the four specimens one measured 3.05 m (10 ft.) long and the remaining three were 1.22 m (4 ft.) long. One of the smaller length specimens served as control specimen, E1.

Specimen E3 measured 1.22 m (4 ft.) in length and had the strand exposed to the environment mimicking an air void and corrosion under environmental conditions. To achieve this, a small section of size 300 mm x 25 mm (12 in. x 1 in.) was cut from the HDPE duct and a small piece of wood was placed, so that when the duct is grouted the grout will fill the duct leaving the strand exposed. Figure 2.3 shows the exposed strand specimen, E3. This specimen was left exposed to the atmosphere for the first 45 days, after which a small quantity of 2% NaCl solution was sprayed only once on the strand to induce corrosion. The two remaining specimens, E2 with a length of 1.22 m (4 ft.) and E4 with a length of 3.05 m (10 ft.) , had 300 mm (1 ft.) long, 25 mm (1 in.) wide and 12.5 mm (1/2 in.) deep grooves to facilitate wet-dry cycling. Figure 2.4 shows the groove for specimen E4. These wet-dry specimens were subjected to 3 days wet (Monday to Wednesday) and 4 days dry (Thursday to Sunday) cycles. Initial wet-dry cycles were started after five days of start of AE with a 2% NaCl solution. This NaCl solution was

maintained for four weeks and then the percentage of NaCl was increased by 2% every week until it reached 10% and was maintained at that level thereafter. A silver chloride (AgCl) reference electrode was embedded into each duct for half-cell potential measurements.

2.5.2. Internally Post-Tensioned Specimens

For the internal PT specimens, the lengths were similar to the external PT specimens. The strand was encased using corrugated poly propylene [PP] grouted ducts with 60.3 mm (2 – 3/8 in.) diameter and 2 mm (1/10 in.) thickness, as opposed to smooth HDPE duct which was used for the external PT specimens. The advantage of having a corrugated duct is that it provides a better bond between the concrete and the duct. The type of grout and water content for the mix remained the same as for external PT specimens.

Chlorides were added in varying percentages in all four specimens. The shorter specimens I1, I2 and I3 had 0.08%, 0.8% and 1.6% chlorides by weight of grout respectively, whereas the longer specimen I4 had 1.6% chlorides by weight of grout. Roughly 16 kg (35 lbs.) of dry grout was required to fill each of the shorter specimens and about 36 kg (80 lbs.) of dry grout was required to fill the longer 3.05 m (10 ft.) specimen. An air pressure powered pump (ChemGrout CG050) was used to pump the grout into the duct which had an output pressure of 1.55 MPa (225 psi). Concrete was then placed around the ducts with a cross-section of 165 mm x 165 mm (6 ½ in. x 6 ½

in.). The cross-section was based on the knowledge that reinforcement is generally located within a structure with a minimum cover of 50 mm (2 in.).

Table 2.1 shows the mix design used for the concrete. Silver chloride (AgCl) reference electrodes were embedded in the grouted ducts for the purpose of half-cell potential [HCP] measurements. Figures 2.5 (a-d) represent internal PT specimens.

2.5.3. Acoustic Emission Equipment

Basic terminology and concepts of AE were discussed in Chapter 1. Stress waves associated with corrosion travel within the strand and grout medium and can be detected by a piezoelectric sensor attached to the surface of the duct or the concrete cover. AE signals can be classified by parameters such as amplitude, duration, rise time, energy, average frequency, RMS, and signal strength that are unique and depend on the magnitude and directionality of the source. The recorded AE parameters can be plotted using special software such as AEWIn (Mistras Group, Inc.) to understand the pattern and to aid in the development of filters to minimize noise and retain meaningful data. The major sources of raw AE are depassivation of steel, corrosion of the strand, cracking in the grout due to expansive nature of corrosion byproducts and noise due to sources such as electrical interference, ground vibrations or wave reflections. After the visual inspection of the raw AE data pattern, two parameters that were used for AE data filtering process are RMS and average frequency. The filters for acceptance limits of the raw AE data are mentioned in Table 2.2. For comparison purposes, the same filters were applied to raw AE data from all the specimens.

Each of the specimens was monitored with two acoustic emission (AE) resonant sensors, 55 kHz with an integral 40 dB pre-amplifier (R6i) as shown in Figure 2.6, (Mistras Group, Inc.). The sensors were strategically located on the specimens to pick up corrosion activity. The sensors were connected to a 16-channel data acquisition system (Sensor Highway II, Mistras Group, Inc.). For the internal PT specimens, one AE sensor was positioned at the center of the top surface of the specimen while the other sensor was positioned on one face of the cross-section between the strand and the grout, as shown in Figure 2.7.

For the external PT specimens, the shorter specimens had a sensor located at 300 mm (1 ft.) from each corner while the longer external PT specimen had sensors located at 910 mm (3 ft.) from corner. The AE sensor location in the shorter external PT specimen is shown in Figure 2.8. The test threshold was set to 40 dB for all channels.

2.6. RESULTS AND DISCUSSIONS

2.6.1. Externally Post-Tensioned Specimens

The ASTM criterion for corrosion of steel in concrete for a silver chloride (AgCl) reference electrode is given in Table 2.2. The half-cell potential [HCP] with respect to time and cumulative signal strength [CSS] with respect to time for each external PT specimen are plotted in Figure 2.9. The HCP measurements were taken with an impedance voltmeter on a weekly basis. In specimen E1, the control specimen, the HCP

measurements indicate that corrosion did not initiate. This agrees with the AE data as minimal AE activity was collected over the span of the test.

In specimens E2 and E4, the wet-dry cycles were initiated five days after installing the AE sensors on the specimens. With an initial NaCl solution concentration of 2% it was observed that corrosion initiated about one week from the beginning of wet-dry cycling, and the half-cell potentials of the specimens went below the threshold of -250 mV by the eighth week of wet-dry cycling. As the NaCl concentration was raised, the corrosion level increased rapidly, which is seen in the half-cell potential measurements as these values went on to become more negative and the recorded AE had significant jumps in signal strength when the NaCl concentration was raised. The AE decreased in the later stages, which may be associated with lower rates of corrosion due to a thin protective layer on the surface of the wires precluding further corrosion of the inner layers. For more corrosion to occur within a reasonable period of time, the salt concentration must be raised. An observation from amplitude vs. time graphs for E2 and E4 shows that majority of the AE activity recorded was during the dry cycling period. This is illustrated in Figure 2.10, where the AE activity in grey region is during the 3 day wet cycling and the AE activity in white region is during the 4 day dry cycling.

E3 is the specimen with the strand exposed to air. Since there are no chlorides in the grout or provision for wet-dry cycling, there was no corrosion activity in the beginning. After 45 days, a small amount of 2% NaCl solution was sprayed on the exposed strand to initiate corrosion. Within two weeks there were visible signs of corrosion, and by the fourth week the HCP measurements fell below the threshold of -250 mV. During this time, the HCP values plummet and there is a related sudden rise in

AE signal strength. The corrosion of the specimens continued even in the absence of the NaCl solution. This can be explained by the work of Feng et al. [25] where it is stated that due to stresses developed in the steel, the rate of re-passivation is much slower and therefore the steel is more susceptible to corrosion. Regular visual inspection of this specimen confirmed this, and it was also apparent in the HCP and AE measurements. Figure 2.11 illustrates visible signs of corrosion in this specimen. A closer look also revealed grout cracking around the strand.

Figures 2.12 and 2.13 are plots of Duration vs. Amplitude and Amplitude vs. Time of each external PT specimen, respectively. From these plots, it can be seen that for specimen E1 there are very few hits of low amplitude and low duration, indicating no active corrosion which is also validated by HCP measurements. The plots for specimens E2, E3, and E4 show there is high AE activity that can be related to active corrosion and is validated by HCP measurements. One interesting feature to notice is, specimens E2 and E3 show a significant number of hits above 60 dB while that is not the case for E4 wherein there are just a few hits higher than 60 dB. Visual inspection of E2 and E3 show grout cracking but no cracking is seen in E4. Therefore it is hypothesized that the grout cracking due to corrosion in this case may be associated with hits of amplitude greater than 60 dB.

2.6.2. Internally Post-Tensioned Specimens

HCP with respect to time and CSS with respect to time for each internal PT specimen are shown in Figure 2.14. For specimen I1 the HCP values are close to -120

mV, indicating a lack of active corrosion. The lack of corrosion activity is reflected in the lack of AE activity, which has less than 50 hits throughout the time the AE signals were recorded. With 0.8% chlorides, the HCP values for specimen I2 are close to -200 mV which is slightly above the threshold of -250 mV, implying that the corrosion level in this specimen is uncertain.

Specimens I3 and I4 vary only in their length, having the same chloride content. The HCP of specimen I3 shows corrosion initiated in the second week and this specimen reached the threshold HCP of -250 mV by the fourth week. In the case of specimen I4, the HCP measurements are in the uncertain region running close to -200 mV. Analysis of the acoustic emission data such as CSS vs. Time, Amplitude vs. Time and intensity analysis indicates active corrosion in both specimen I3 and I4. Some potential reasons to explain the HCP measurements of specimen I4 are: uneven distribution of chlorides in the specimen, leading to lesser corrosion occurring in the region where the reference electrode is located; a lack of contact between the reference electrode and the strand or grout; internal air pockets; or a faulty reference electrode. One method to cross check the performance of this reference electrode in I4 is by measuring the potential between it and another reference electrode preferably silver chloride, but to perform this action the reference electrode has to be removed from the specimen first. This illustrates the advantage of using AE as an SHM method to detect corrosion in PT structures because conventional electrochemical measurements can sometimes be misleading. The advantage of HCP measurements is the simplicity of the technique; however it has been reported that HCP can show no corrosion when corrosion actually is occurring and vice versa [26, 27].

Figures 2.15 and 2.16 are plots of Duration vs. Amplitude and Amplitude vs. Time of each individual internal PT specimen respectively. Here it can be seen that the control specimen I1 has the least recorded AE activity indicating no active corrosion which is in accordance with HCP measurements. Specimen I3 and I4 have very high AE activity which can be related to corrosion, while specimen I2 has lesser AE activity as compared to I3 and I4 indicating lesser active corrosion, all of which is in accordance with HCP measurements.

2.6.3. Intensity Analysis

Intensity Analysis is a damage quantification methodology for AE data. It is used to aid in the understanding of the degree of damage and is a statistically based method related to AE signal strength, which is used to compute Historic Index and Severity [28]. Intensity Analysis is a plot of Historic Index on the x-axis and Severity on y-axis. Historic Index, $H(t)$, is the measure of change of signal strength whereas Severity (S_r) is an average of the largest 50 signal strength values. Equations to calculate Historic Index and Severity are:

$$H(t) = \frac{N}{N-K} \cdot \left(\frac{\sum_{i=K+1}^N S_{oi}}{\sum_{i=1}^N S_{oi}} \right) \quad (\text{Eq.2.1})$$

$$S_r = \frac{1}{J} \cdot \{ \sum_{m=1}^J S_{om} \} \quad (\text{Eq.2.2})$$

where, N is the number of hits, S_{oi} and S_{om} are signal strength and K and J are empirical constants based on material under consideration. The constants K & J depend on N , and for concrete are often given as a) $K = N/4$ if $N \leq 50$; b) $K = N-30$ if $51 \leq N \leq 200$; c)

$K=0.85N$ if $201 \leq N \leq 500$; d) $K = N-75$ if $N \geq 501$; e) $J= 0$ for $N < 50$; and f) $J=50$ for $N \geq 50$. To portray the level of damage, an Intensity Analysis chart is subdivided into regions where each region corresponds to a particular level of damage.

Figure 2.17 and 2.18 show the intensity analysis charts for external and internal PT specimens respectively. For external PT specimens, the control specimen E1 lies in the no damage region; E2 and E3 are in the severe damage region, while E4 lies in the depassivation region. Though E2 and E4 differ only in length, E2 is in the severe damage region whereas E4 is in the depassivation region of the intensity analysis chart. Visual inspections reveal severe grout cracking around E2 and E3, but in the case of E4 not much grout cracking is observed even though the corrosion levels are similar to E2 according to HCP measurements. Lesser cracking results in AE with lesser signal strength which in turn affects the intensity analysis charts.

For internal PT specimens, the coordinates of specimen I1 are at unity indicating no corrosion damage. This is because this specimen recorded no active corrosion as per HCP and the numbers of AE hits recorded during the entire period of test are less than 50. Specimen I2 is in the depassivation region and in the verge of entering into to cracking region, while specimens I3 and I4 with the highest NaCl concentration are in the severe damage region.

2.6.4. Source Location

An interesting feature in AE is its ability to locate the source of damage. Source location was adopted for two externally PT specimens, namely specimens E2 and E3. It was observed that most of the AE activity that was recorded for E2 came from the groove

where in wet-dry cycles were performed and for E3 came from the region where the strand was left exposed. Figure 2.19 shows the source location in specimens E2 and E3.

2.7. CONCLUSIONS

Corrosion was induced in both internal and external PT specimens. Long term monitoring of corrosion was performed on the specimens by half-cell potential and acoustic emission monitoring. Conclusions are:

- a) Acoustic Emission is not only successful in detecting and quantifying damage in PT structures due to corrosion, but may detect the corrosion process prior to the conventional electrochemical measurements. Importantly, it can be effectively used where there is no provision for electrochemical measurements.
- b) Intensity Analysis proved to be useful to determine the degree of damage in the specimens. The results were in accordance with the HCP measurements.
- c) Appropriate filters need to be utilized to minimize noise.
- d) AE can be a very efficient monitoring method to detect corrosion in PT concrete structures in real time.

REFERENCES

1. FHWA – Post Tensioning Tendon Installation And Grouting Manual, 2004
2. Durability And Sustainability of Concrete Bridges, PCI Presentation, 2009
3. Podolny, Walter Jr., 1992,”Corrosion of prestressing steels and its mitigation”, PCI Journal, Volume: 37, Issue: 5.
4. Woodward, R.J. and William, F.W., 1988,”Collapse of Ynys – y – Gwas Bridge, West Glamorgan,” Proceedings of Institute of Civil Engineers, Part 1, Volume.84,pp.635-669.
5. Florida Department of Transportation,2001a,”Mid bay Bridge Post – Tensioning Evaluation,” Final Report, Corven Engineering, Inc., FDOT, Tallahassee, FL,2622pp.
6. Florida Department of Transportation,2001b,”Sunshine Skyway Bridge Post – Tensioned tendons Investigation,” Parsons Brinckerhoff Quade and Douglas, Inc., FDOT, Tallahassee, FL.
7. Electrochemical Characterization and Time Variant Structural Realibility Assessment of Post – Tensioned Segmental Concrete Bridges, Dissertation, Radhakrishna.G. Pillai, 2009.
8. Evaluation of External Post Tensioned Tendons Using Vibration Signatures, Dissertation, Jun Ki Lee, 2007
9. Dickson. T.J., Tabatabai. H., Whiting. D.A., “Corrosion Assesment of a 34 Year Old Precast Post – tensioned Concrete Girder”, PCI Journal, Nov – Dec 1993.
10. Federal Highway Administration (FHWA), 2011,”Elevated Chloride Levels in Sika Grout 300 PT Cementitious Grout”, Memorandum.

11. Li, Z., Zudnek, A., Landis, E., Shah, S., 1998, "Application of Acoustic Emission Technique to Detection of Reinforcing Steel Corrosion in Concrete," *ACI Materials Journal*, 95(1),68 – 76.
12. Ziehl, P., 2008,"Application of Acoustic Emission Evaluation for Civil Infrastructure," *SPIE Smart Structures and Materials and Nondestructive Evaluation and Health Monitoring*, San Diego, CA, 9 pp., March 9 – 13.
13. Mangual, J., ElBatanouny, M. K., Ziehl, P., and Matta, F. (2013). "Acoustic-Emission-Based Characterization of Corrosion Damage in Cracked Concrete with Prestressing Strand". *ACI Materials Journal*, 110(1), 89.
14. Mangual, J., ElBatanouny, M.K., Ziehl, P., and Matta, F. (2012). "Corrosion Damage Quantification of Prestressing Strands Using Acoustic Emission." *ASCE Journal of Materials in Civil Engineering*, in press.
15. Assouli B, Simescu F, Debicki G and Idrissi H. Detection and identification of concrete cracking during corrosion of reinforced concrete by acoustic emission coupled to the electrochemical techniques. *NDT & E International*. 2005; 38: 682-9.
16. Yuyama S, Yokoyama K, Niitani K, Ohtsu M and Uomoto T. Detection and evaluation of failures in high-strength tendon of prestressed concrete bridges by acoustic emission. *Construction and Building Materials*. 2007; 21: 491-500.
17. Ohno K and Ohtsu M. Crack classification in concrete based on acoustic emission. *Construction and Building Materials*. 2010; 24: 2339-46.
18. Kawasaki Y, Tomoda Y and Ohtsu M. AE monitoring of corrosion process in cyclic wet–dry test. *Construction and Building Materials*. 2010; 24: 2353-7.

19. Lyons R, Ing M and Austin S. Influence of diurnal and seasonal temperature variations on the detection of corrosion in reinforced concrete by acoustic emission. *Corrosion Science*. 2005; 47: 413-33.
20. Cullington DW, MacNeil D, Paulson P and Elliott J. Continuous acoustic monitoring of grouted post-tensioned concrete bridges. *NDT & E International*. 2001; 34: 95-105.
21. Perrin M, Gaillet L, Tessier C and Idrissi H. Hydrogen embrittlement of prestressing cables. *Corrosion Science*. 2010; 52: 1915-26.
22. Idrissi H and Limam A. Study and characterization by acoustic emission and electrochemical measurements of concrete deterioration caused by reinforcement steel corrosion. *NDT & E International*. 2003; 36: 563-9.
23. Ohtsu M and Tomoda Y. Phenomenological model of corrosion on process in reinforced concrete identified by acoustic emission. *ACI Mater J*. 2008; 105: 194-9.
24. Ramadan S, Gaillet L, Tessier C and Idrissi H. Detection of stress corrosion cracking of high-strength steel used in prestressed concrete structures by acoustic emission technique. *Applied Surface Science*. 2008; 254: 2255-61.
25. Feng X, Tang Y and Zuo Y. Influence of stress on passive behavior of steel bars in concrete pore solution. *Corrosion Science*. 2011; 53: 1304-11.
26. Broomfield, John P., "Corrosion of Steel in Concrete", Second Edition, 2007.
27. Song, G., Shayan, A., "Corrosion of Steel in Concrete – State of the art Review", ARRB Transportation Research, Review Report 4, July 1998.
28. Nair A and Cai CS. Acoustic emission monitoring of bridges: Review and case studies. *Engineering Structures*. 2010; 32: 1704-14.

29. Xu, J. (2008). “Nondestructive evaluation of prestressed concrete structures by means of acoustic emission monitoring”, Dissertation, Dept. of Civil Engineering, Univ. of Auburn, Auburn, Alabama.
30. Prestressed Concrete, Edward Nawy, Fifth Edition
31. Evaluation of External Post Tensioned Tendons Using Vibration Signatures, Dissertation, Jun Ki Lee, 2007
32. Hamilton. H.R., Wheat. H.G., Breen. J.E., Frank. K.H., “Corrosion testing of Grout for Post-tensioning Ducts and Stay Cables”, Journal of Structural Engineering, Feb 2000.
33. West. J.S., Breen. J.E., Vignos. R.P., “Evaluation of Corrosion Protection for Internal Prestressing Tendons in Precast segmental bridges”, PCI Journal.
34. Salas. R.M., Schokker. A.J, West. J.S., Breen. J.E., Kreger. M.E., “Corrosion Risk of Bonded Post Tensioned Concrete Elements”, PCI Journal, Jan – Feb 2008.

Table 2. 1: Concrete mix design for internal PT specimens.

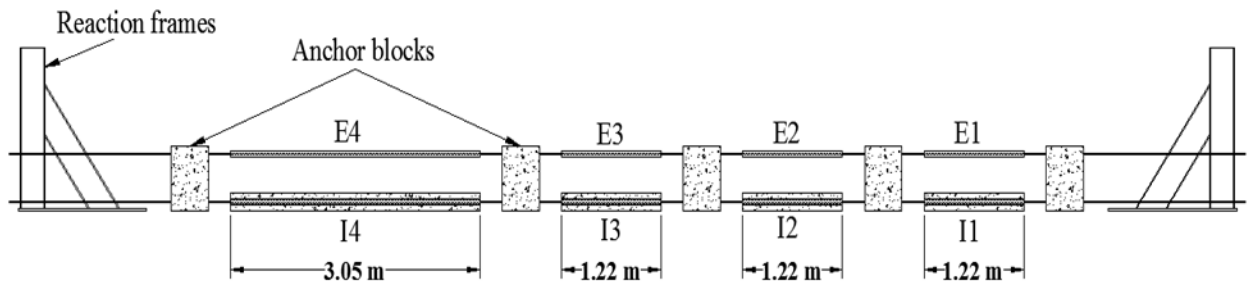
Concrete Mix Design	
Cement	370 kg/m ³
Fine Aggregates	675 kg/m ³
Coarse Aggregates	1240 kg/m ³
Water	140 kg/m ³

Table 2. 2: AE waveform filters

Parameter	Acceptance Limits
RMS (V)	0.0002 to 0.0004
Average Frequency (kHz)	30 to 100

Table 2. 3: ASTM corrosion for AgCl reference electrode (Broomfield, 2007)

Potential Against AgCl Electrode	Corrosion Condition
> -100 mV	Low Risk (10% probability of corrosion)
-100 to -250 mV	Intermediate corrosion risk
< -250 mV	High Corrosion risk (90% probability)
< -400 mV	Severe Corrosion Damage



Designation	Type	Designation	Type
E1	Control	I1	0.08% Cl
E2	Wet-Dry cycle	I2	0.8% Cl
E3	Exposed Strand	I3	1.6% Cl
E4	Wet-Dry Cycle	I4	1.6% Cl

Figure 2. 1: General experimental layout for PT specimens



(a)



(b)



(c)



(d)

Figure 2. 2: External Post-Tensioned Specimens: (a) Control, E1; (b) Wet-dry 4 ft, E2; (c) Exposed Strand, E3; and (d) Wet-dry 10ft, E4



Figure 2. 3: Top view of specimen E3

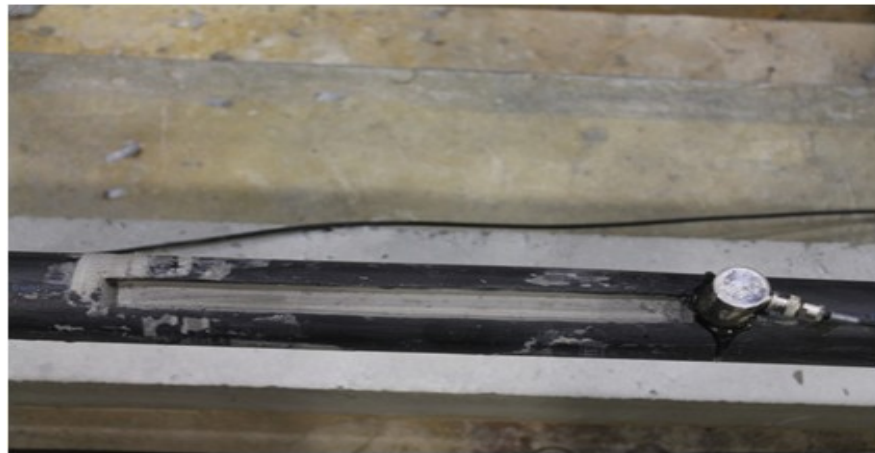
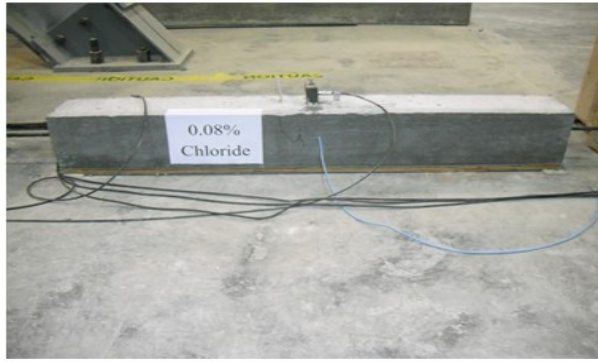
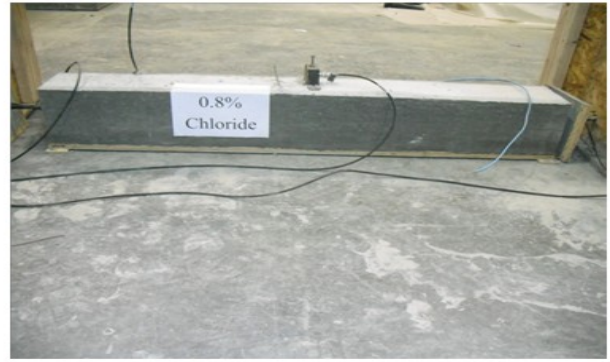


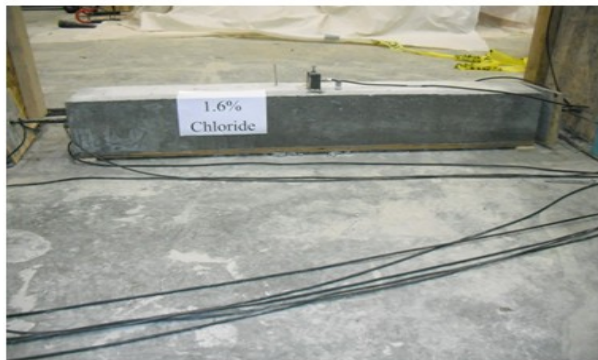
Figure 2. 4: Groove to facilitate wet-dry cycles



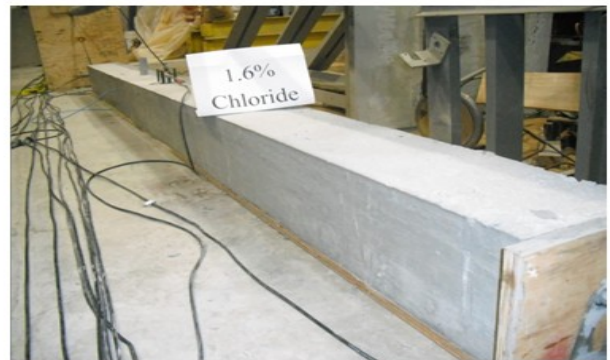
(a)



(b)



(c)



(d)

Figure 2. 5: Internal PT Specimens: (a) 0.08% Cl, I1; (b) 0.8% Cl, I2; (c) 1.6% Cl, 4ft, I3; and (d) 1.6% Cl, 10ft, I4



Figure 2. 6: R6i AE sensor (Mistras Group, Inc.)

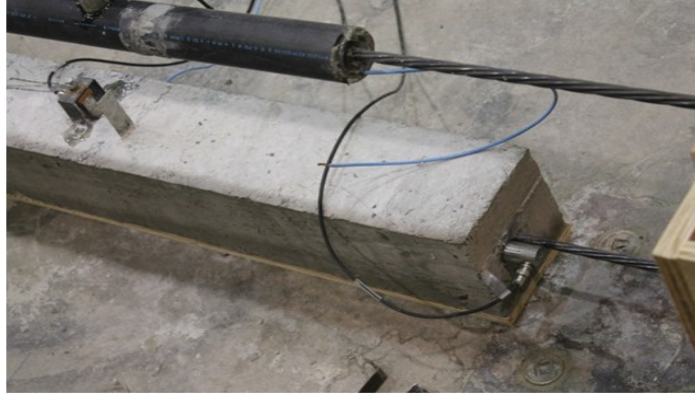


Figure 2. 7: Positioning of sensors on internal PT specimens



Figure 2. 8: Positioning of sensors on external PT specimens

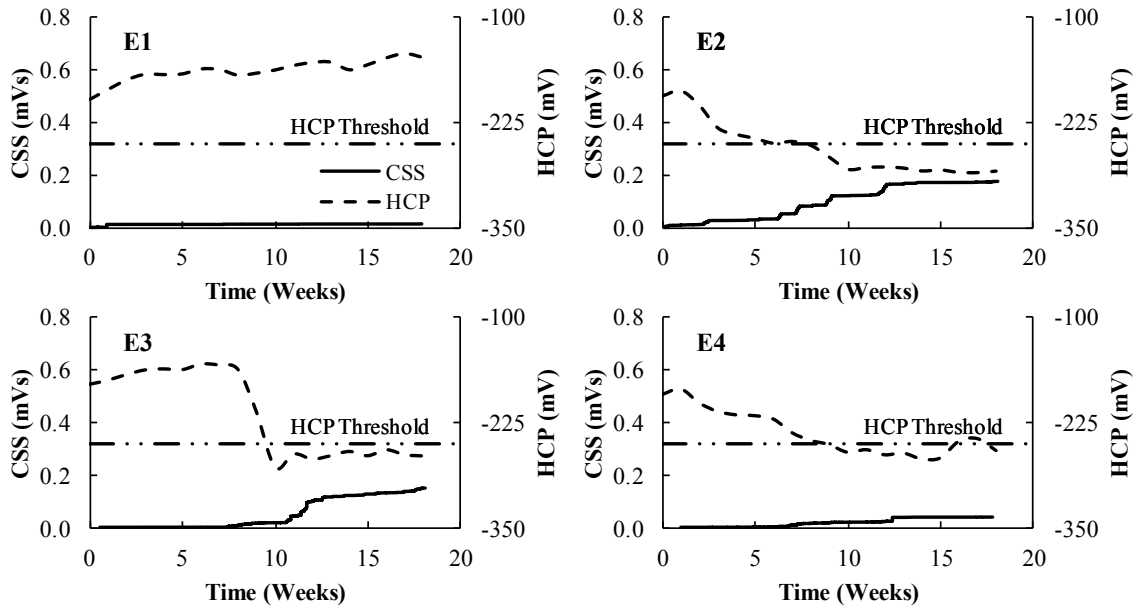
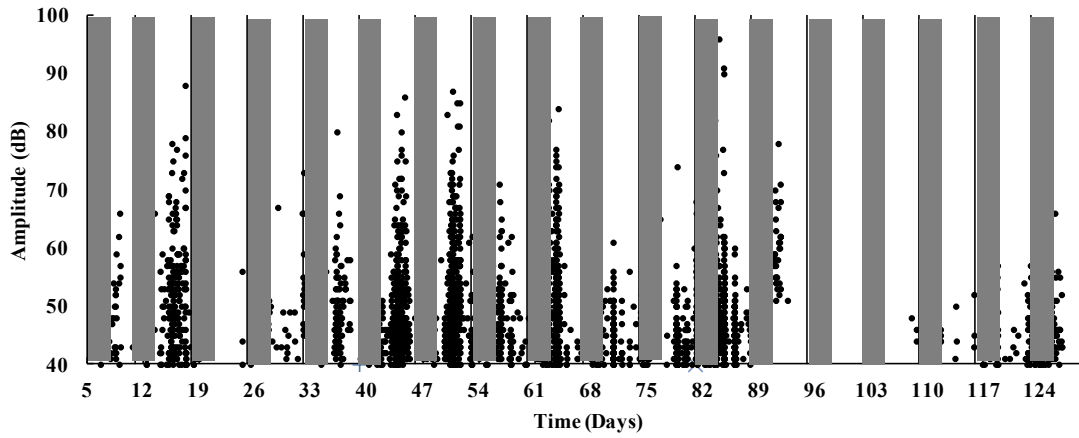
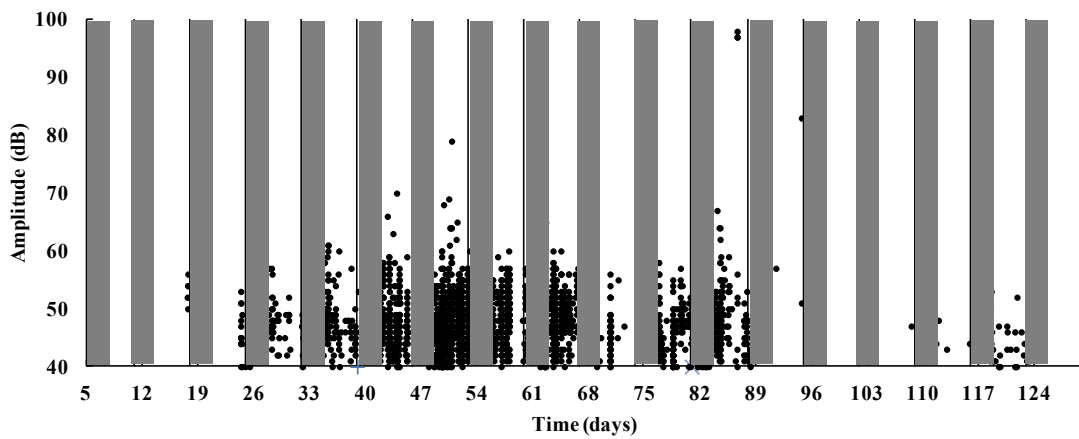


Figure 2. 9: CSS vs. time and HCP vs. time for external PT specimens



(a)



(b)

Figure 2. 10: Amplitude vs. time for specimens a) E2, b) E4 illustrating corrosion in dry cycling

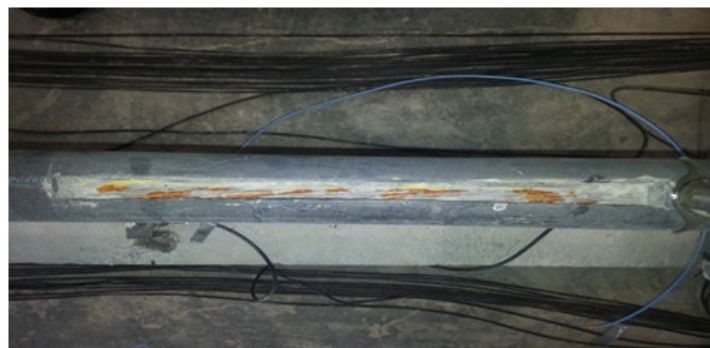


Figure 2. 11: Visible corrosion in specimen E3

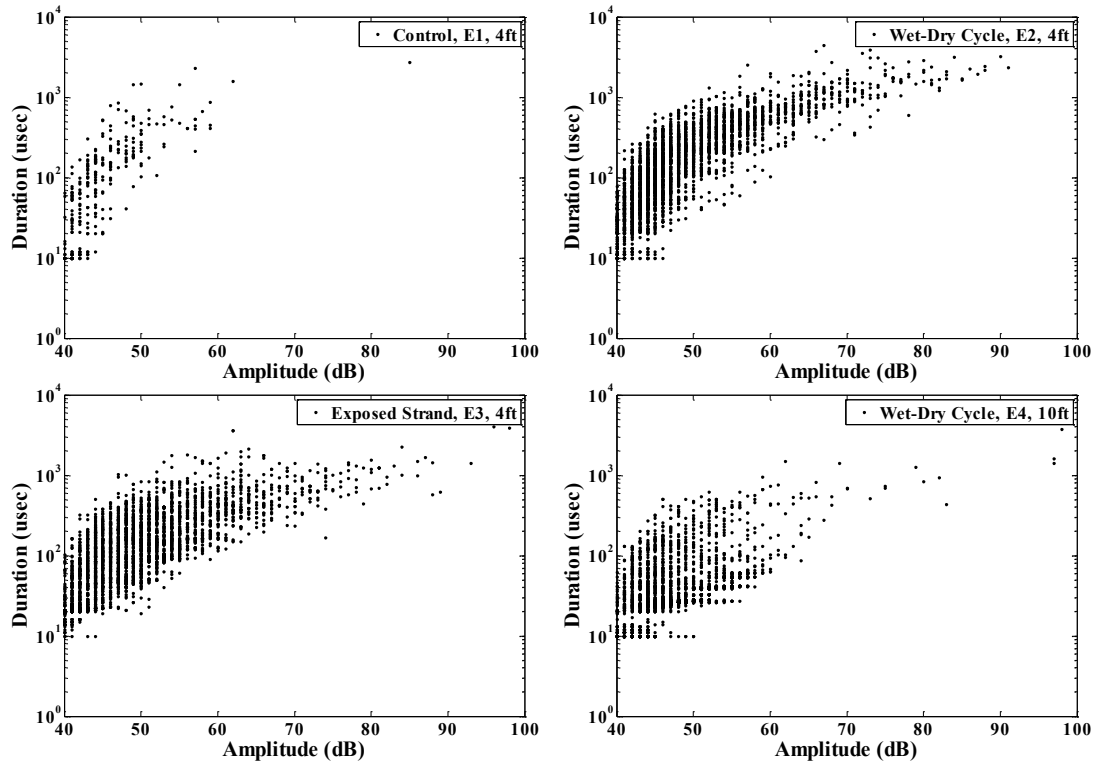


Figure 2. 12: Duration vs. Amplitude for external PT specimens

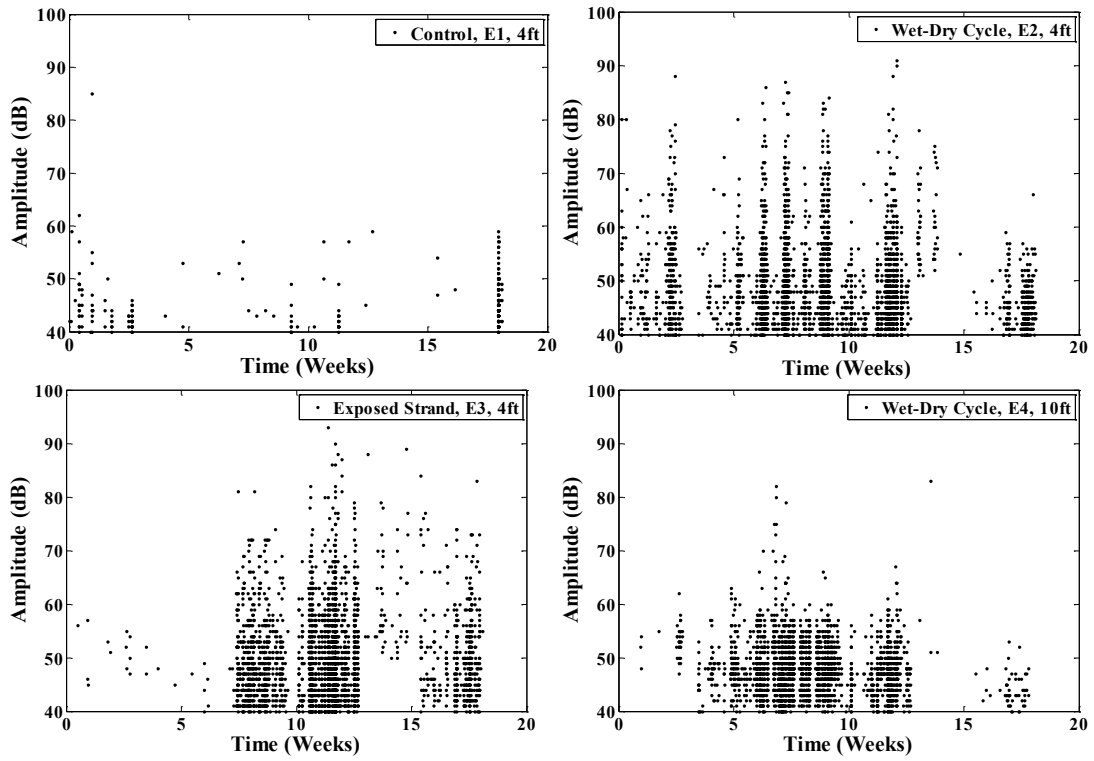


Figure 2. 13: Amplitude vs. time for external PT specimens

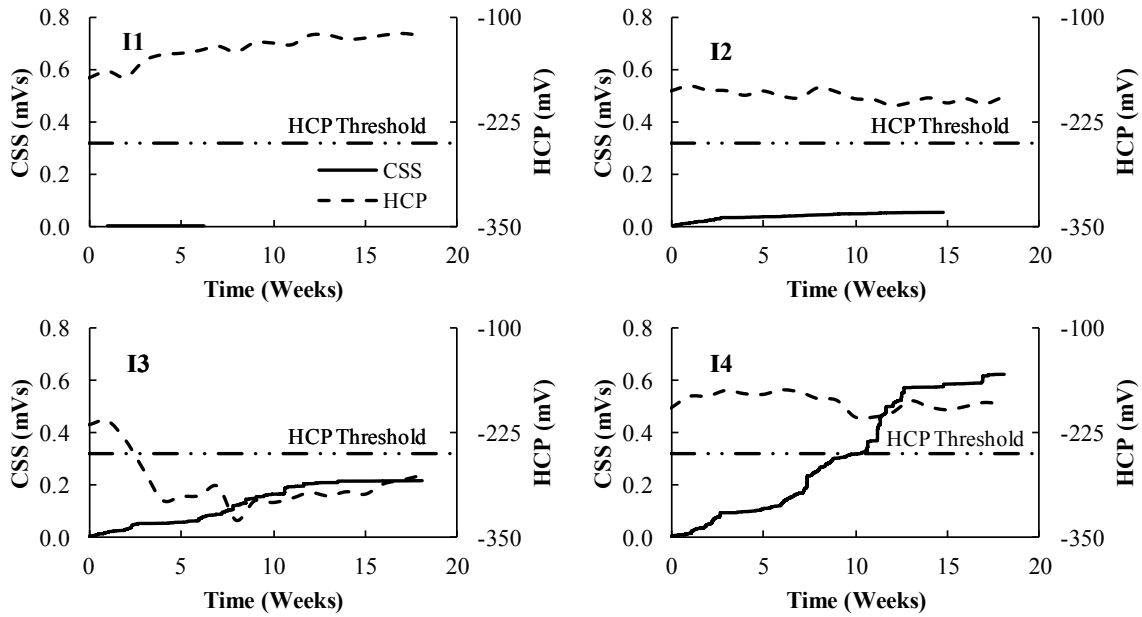


Figure 2.14: CSS vs. time and HCP vs. time for internal PT specimens

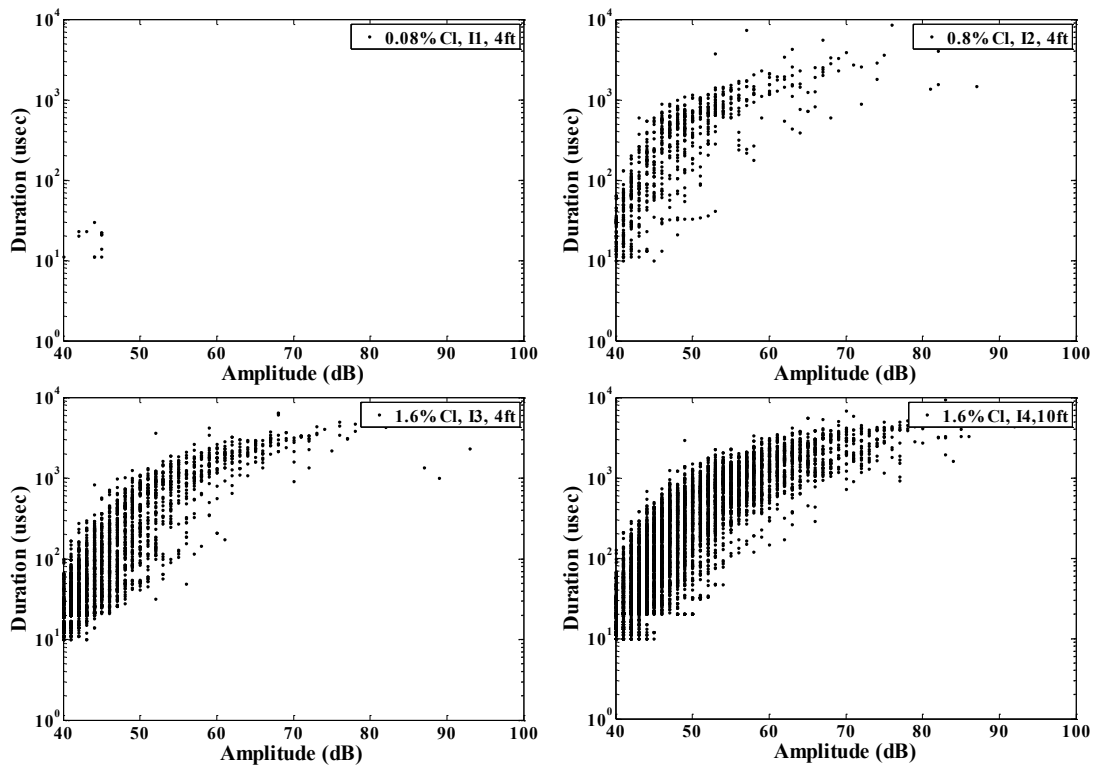


Figure 2.15: Duration vs. Amplitude for internal PT specimens

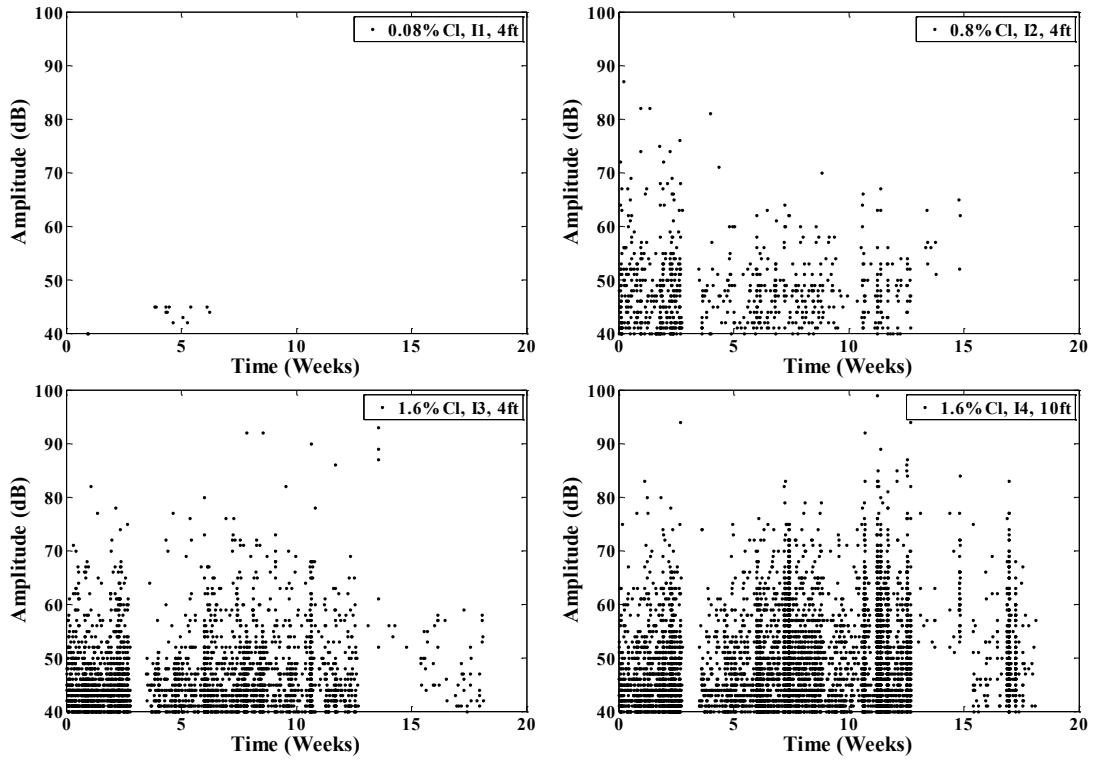


Figure 2. 16: Amplitude vs. time for internal PT specimens

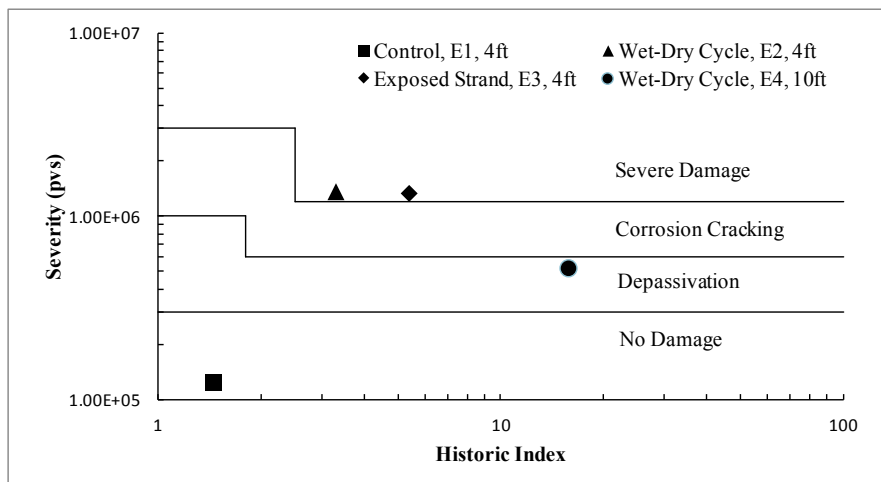


Figure 2. 17: Intensity analysis chart for external PT specimens

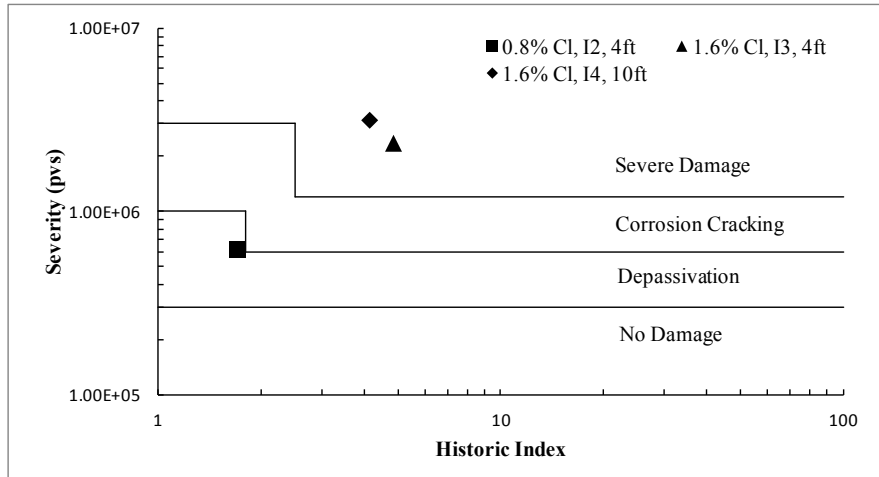


Figure 2. 18: Intensity analysis chart for internal PT specimens

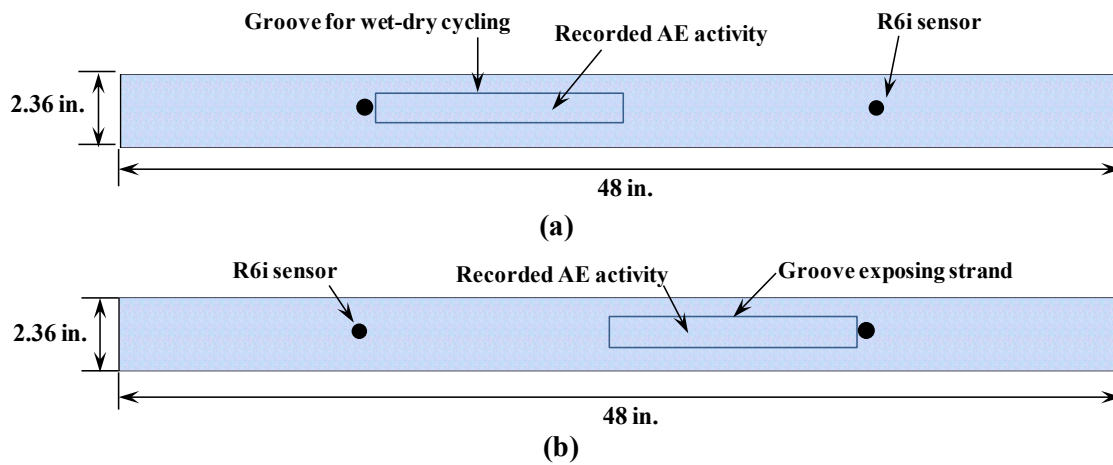


Figure 2. 19: Source location for (a) specimen E2 (b) specimen E3

CHAPTER – 3

A PRELIMINARY INVESTIGATION OF BIOPOLYMER DOPED CEMENT MORTARS FOR USE IN STRUCTURAL RESTORATION¹

¹Aditya Appalla, Nirupam Aich, Navid Saleh, Paul Ziehl

3.1. ABSTRACT

Small scale repair and restoration of concrete structures is often approached with cement mortar patch working. Polymeric additive of about 10 – 20% by weight of cement are often substituted in the mortar mix to enhance the properties of the patch work. But due to the very high cost of the polymeric additives, the overall cost of patch work becomes very expensive. Other drawbacks such as toxicity, odor, flammability, and rapid hardening prevent wider applications of these materials. Newer replacements for these polymers are needed that are cheaper and are yet efficient in enhancing the properties of the patch mortar. In this investigation dopamine hydrochloride was doped into cement mortar by a very minimal quantity of 0.5% weight of cement. This quantity is much less than normally utilized and therefore the expense of the mortar is minimized. Two inch mortar cubes were cast with dopamine mortar and compression testing was conducted at seven and twenty eight days. Results indicate that dopamine can provide high early strength as compared to regular mortar making them suitable as additives for patching or repair works. An added and intriguing benefit is a noticeable improvement in the load-displacement behavior of the mortar.

Keywords: Dopamine hydrochloride, patch work, cement, biopolymers

3.2. INTRODUCTION

Concrete is said to be durable when it can withstand weathering action due to external factors such as abrasion, chemical attack, or any other similar deterioration processes. With the aging and repeated use of infrastructure, there is an obvious reduction in the durability of the structure. Cracking and spalling in concrete structures are two durability issues that are already well known, and its repair is necessary to restore the durability. Research has proposed many different methods of structural repair [1 – 7]. Some of the methods include metal fittings, fiber retrofitting [GFRP and CFRP], and patch working by regular cement mortars. While metal fittings and fiber retrofitting are used mostly for heavily damaged structures, patch working remains the prominent and chosen method when it comes to repair of small scale cracking and spalling. This technique is relatively cheaper, simpler, and faster when compared to the other methods.

To meet the demands of heavy traffic, most real time applications of patch working require that the patch work be fast setting, attain high early strength, and demonstrate considerable durability. To meet these demands, additives are utilized in the mortar mix to enhance its properties. Additives such as GGBS, silica fume, fly ash, magnesium phosphate and other polymeric compounds are some of the standard choices. The typical enhanced properties that are achieved are; up to four fold increases in compressive strength followed by a corresponding increase in tensile and flexural strength, lower permeability, faster curing, high early strength, and excellent durability.

Of the various types of additives, polymeric additives have gained significant importance over the last 35 years [8 – 12]. Polymers for use in cement were first

developed in 1950's, but it was during the 1970's when their use became commercial. Mortar made with polymer is known as polymer modified mortar [PMM] and concrete made with polymer is known as polymer modified concrete [PMC]. Polymers can be available in various forms such as liquid resins, latexes, powder or water soluble, and the choice depends on the use, cost and required enhancements. Some examples of polymers are vinyl acetate ethylene, styrene butadiene, styrene acrylic and acrylic.

Though there are many advantages to using PMM, there are still some disadvantages that retard usage of such materials [10]. First is the cost factor. The amount of polymer that is usually required is 10 – 20% the weight of cement, and the cost of these polymers ranges from anywhere between 10 and 100 times the cost of cement. Assuming a specific gravity of 2.5 times that of cement, the cost per unit volume of polymer is still very high. Some other drawbacks are odor, toxicity and inability to withstand fire and a fierce competition from rapid hardening cement types which are relatively much cheaper and thus pose a threat to the use of polymers.

Newer polymeric compounds are needed, that are cheaper, easier to handle and provide the necessary improvements in the mortar. Dopamine hydrochloride, commonly known as dopamine, is a non-toxic, odorless, non-flammable and inexpensive naturally occurring biopolymer. In this chapter we study the effect of dopamine on the properties of cement mortar. Mortar specimens that contained dopamine were tested at seven and twenty eight days to prove that dopamine can serve as a replacement to the already existing polymers in cement mortar for repair purposes.

3.3. MATERIALS AND PREPRATION

Materials required for the investigation were Dopamine Hydrochloride and Tris Buffer Saline Solution (both obtained from Sigma Aldrich), White Type I Cement, and sand conforming to ASTM C778. The tris buffer solution was diluted 20 times with pH maintained at 8.5.

3.4. EXPERIMENTAL PROCEDURE

Two inch cement mortar cubes were cast in accordance with ASTM C109 and ASTM C305 for compression testing at seven and twenty eight days. The ratio of cement to sand was 1:2.75. Two separate batches, one control and another with dopamine were cast. For control specimens, potable water with a water to cement ratio of 0.485 was added into the dry mortar mix, and for the dopamine mortar specimens, diluted tris buffer solution of the same ratio was added instead of portable water. A dopamine content of 0.5% weight of cement was added to the tris solution and mixed for one minute with a magnetic stirrer before immediately adding the tris solution into the mortar mix. This mixing time of one minute and the mortar mixing procedure in ASTM C305 were strictly followed. The contents were mixed thoroughly with an electric mixer and placed in metal molds. A very thin layer of mold release agent was applied on the internal wall of the mold to facilitate ease of removal of cubes after the curing process.

Excess release agent was avoided because the reaction between release agent and dopamine is uncertain. The molds were then covered in mildly wet burlap and placed in

boxes with water filled up to half the height of the box and then the whole box was covered with a plastic sheet to minimize potential loss of moisture. The temperature and humidity inside the box was recorded at 65°F and 70% respectively. Curing was done for 24 hours after which the specimens were removed from molds and put in a container with water and lime powder for further curing for seven and twenty eight days. The quantity of lime was maintained at 3 grams/liter of water. When placing the cubes in the lime water, the cubes must be sufficiently distant from each other at least ½ inches apart. The cubes tend to stick to each other if they are touching or stacked on top of one another. The cubes were then tested at seven and twenty eight days on an MTS 810 testing machine using displacement control mode of loading. The rate of displacement loading of the machine was maintained at 0.025 in/min.

3.5. TEST RESULTS

At the age of seven days, the dopamine mortar specimens averaged strength of 38 MPa (5,450 psi) where the control specimens averaged strength of (33 MPa) 4,790 psi. This is 13.8% higher strength at seven days. Table 3.1 and 3.2 are the strengths obtained for dopamine and control specimens respectively at the age of seven days. The 28 days average strength for dopamine mortar was 39 MPa (5,690 psi) whereas for regular mortar specimens it is 42 MPa (6,050 psi). Table 3.3 and 3.4 show the twenty eight day strength results for dopamine and control specimens respectively. An important observation at seven days testing was load vs. displacement graphs which showed a notably improved load-deformation behavior in specimens with dopamine. Figure 3.1 and 3.2 are the

graphs of load vs. displacement for 7 days and 28 days for dopamine mortar specimens and Figure 3.3 and 3.4 show load vs. displacement curves for control specimens at 7 and 28 days.

3.6. SEM IMAGING RESULTS

Figure 3.5 provides with the microstructure comparison of a biopolymer reinforced concrete with the conventional concrete having no biopolymer. Figure 3.5a shows typical surface of a traditional concrete while polymeric matrix evolving on the surface of concrete is observed in Figure 3.5(b-c). Uniform and well spread polymeric matrix adhering to the concrete (figure 3.5b) can offer the increased adhesion properties to the concrete structure in 7 days. On the other hand, figure 3.5c disruption of the polymeric film which may explain not so much increase during 28 days test.

3.7. CONCLUSIONS

The preliminary compression tests on mortar specimens containing dopamine show that this biopolymer has the potential to be used as an additive into cement mortars for patch working. Some of the advantages of dopamine as an additive are:

- a. From the compression test results for seven and twenty eight days, it can be seen that dopamine can help to achieve a very high early strength in the mortar. The seven day compressive strength for dopamine mortar is very close to the 28 day strength of regular mortar.

- b. Dopamine is only required in a very minute quantity of 0.5% weight of cement and also dopamine is an inexpensive biopolymer. This is a huge benefit as the costs involved for using polymers can be significantly lowered.
- c. From the load vs. displacement curves for dopamine mortar specimens, it is observed that there is a significant increase in the load-deformation as compared to the control specimens.
- d. Dopamine is non-toxic, odorless, and non-flammable. Therefore special requirements are not required for handling.

The twenty eight day strength for dopamine mortar specimens is slightly lower than that of the control. A possible explanation for this could be the rupture of dopamine film which is seen in the SEM images. Dopamine shows some promise as an additive for use in cement mortar for structural repair. Further research with this material is needed to better understand the behavior of this material under different conditions of temperature, moisture, and chemical reactivity.

REFERENCES

1. Pellegrino C, Porto Fd and Modena C. Rehabilitation of reinforced concrete axially loaded elements with polymer-modified Cementitious mortar. *Construction and Building Materials*. 2009; 23: 3129-37.
2. Martinola G, Meda A, Plizzari GA and Rinaldi Z. Strengthening and repair of RC beams with fiber reinforced concrete. *Cement and Concrete Composites*. 2010; 32: 731-9.
3. Raupach M. Patch repairs on reinforced concrete structures – Model investigations on the required size and practical consequences. *Cement and Concrete Composites*. 2006; 28: 679-84.
4. Sharif A, Rahman MK, Al-Gahtani AS and Hameeduddin M. Behaviour of patch repair of axially loaded reinforced concrete beams. *Cement and Concrete Composites*. 2006; 28: 734-41.
5. Qiao F, Chau CK and Li Z. Property evaluation of magnesium phosphate cement mortar as patch repair material. *Construction and Building Materials*. 2010; 24: 695-700.
6. Pacheco-Torgal F, Abdollahnejad Z, Miraldo S, Baklouti S and Ding Y. An overview on the potential of geopolymers for concrete infrastructure rehabilitation. *Construction and Building Materials*. 2012; 36: 1053-8.
7. Mechtcherine V. Novel cement-based composites for the strengthening and repair of concrete structures. *Construction and Building Materials*. 2013; 41: 365-73.
8. Ohama Y. Recent progress in concrete-polymer composites. *Advanced Cement Based Materials*. 1997; 5: 31-40.

9. Ohama Y. Polymer-based admixtures. *Cement and Concrete Composites*. 1998; 20: 189-212.
10. Fowler DW. Polymers in concrete: a vision for the 21st century. *Cement and Concrete Composites*. 1999; 21: 449-52.
11. Gorninski JP, Dal Molin DC and Kazmierczak CS. Study of the modulus of elasticity of polymer concrete compounds and comparative assessment of polymer concrete and portland cement concrete. *Cement and Concrete Research*. 2004; 34: 2091-5.
12. Aggarwal LK, Thapliyal PC and Karade SR. Properties of polymer-modified mortars using epoxy and acrylic emulsions. *Construction and Building Materials*. 2007; 21: 379-83.
13. Decter MH. Durable concrete repair — Importance of compatibility and low shrinkage. *Construction and Building Materials*. 1997; 11: 267-73.

Table 3.1: Seven days compressive strength for dopamine mortar specimens

Cube	Weight (grams)	Avg & Std Dev (Weight)	Strength (psi)	Avg & Std Dev (Strength)
7A1	285	285.6	5415	5450
7A2	290	2.88	5400	279
7A3	285		5100	
7A4	286		5880	
7A5	282		5450	

Table 3.2: Seven days compressive strength for control mortar specimens

Cube	Weight (grams)	Avg & Std Dev (Weight)	Strength (psi)	Avg & Std Dev (Strength)
7C1	283	287	4670	4790
7C2	290	3.11	4535	201
7C3	290		5040	
7C4	284		4760	
7C5	286		4930	

Table 3.3: Twenty eight days compressive strength for dopamine mortar specimens

Cube	Weight (grams)	Avg & Std Dev (Weight)	Strength (psi)	Avg & Std Dev (Strength)
28A1	285	286	5795	5690
28A2	282	3.08	5340	245
28A3	285		5970	
28A4	290		5800	
28A5	288		5550	

Table 3.4: Twenty eight days strength for control mortar specimens

CUBE	Weight (gm)	Avg & Std Dev (Weight)	Strength (psi)	Avg & Std Dev (Strength)
28C1	287	287.8	6010	6050
28C2	287	2.95	6050	430
28C3	289		6620	
28C4	284		6140	
28C5	292		5420	

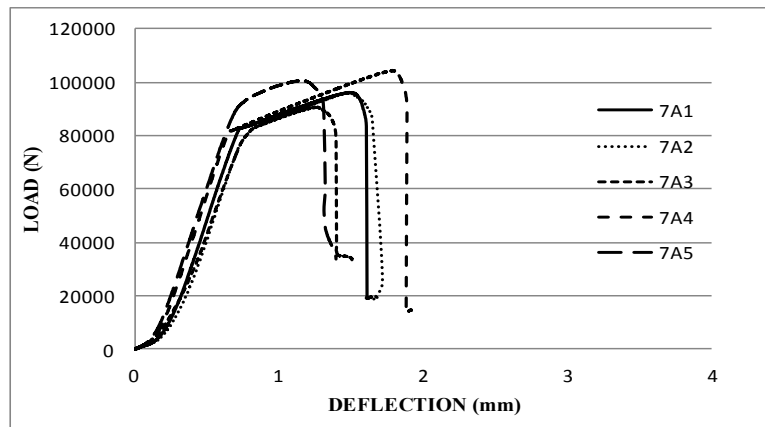


Figure 3.1: Seven days load vs. deflection curves for dopamine mortar specimen

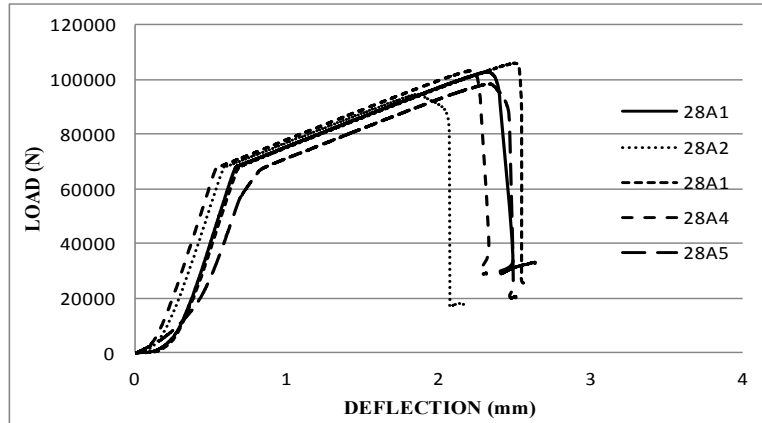


Figure 3.2: Twenty eight days load vs. deflection curves for dopamine mortar specimens

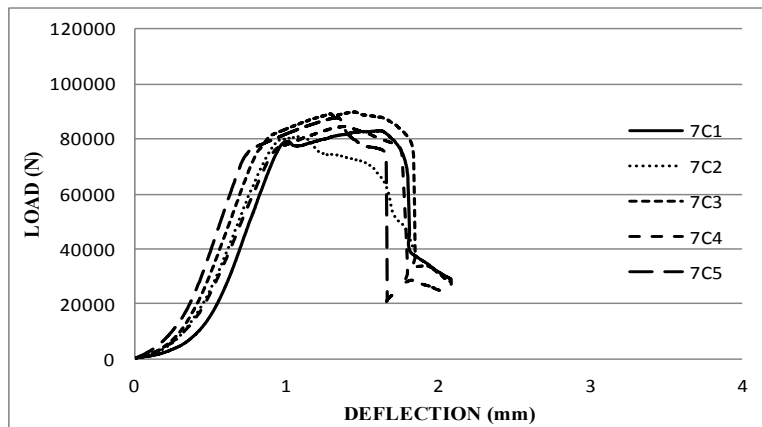


Figure 3.3: Seven days load vs. deflection curves for control specimens

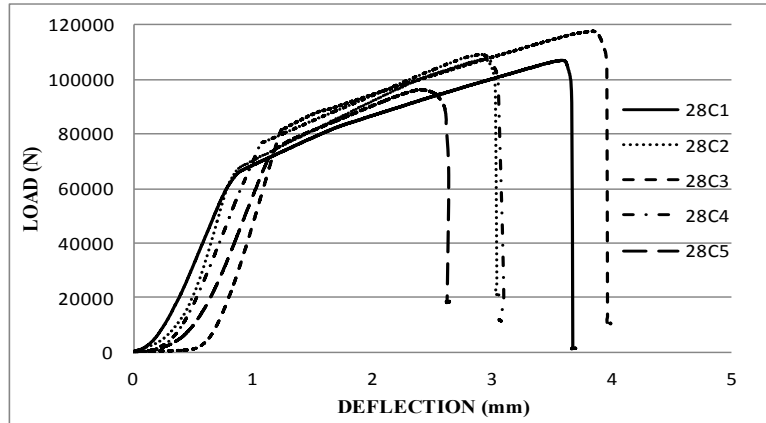


Figure 3.4: Twenty eight days load vs. deflection curves for control specimens

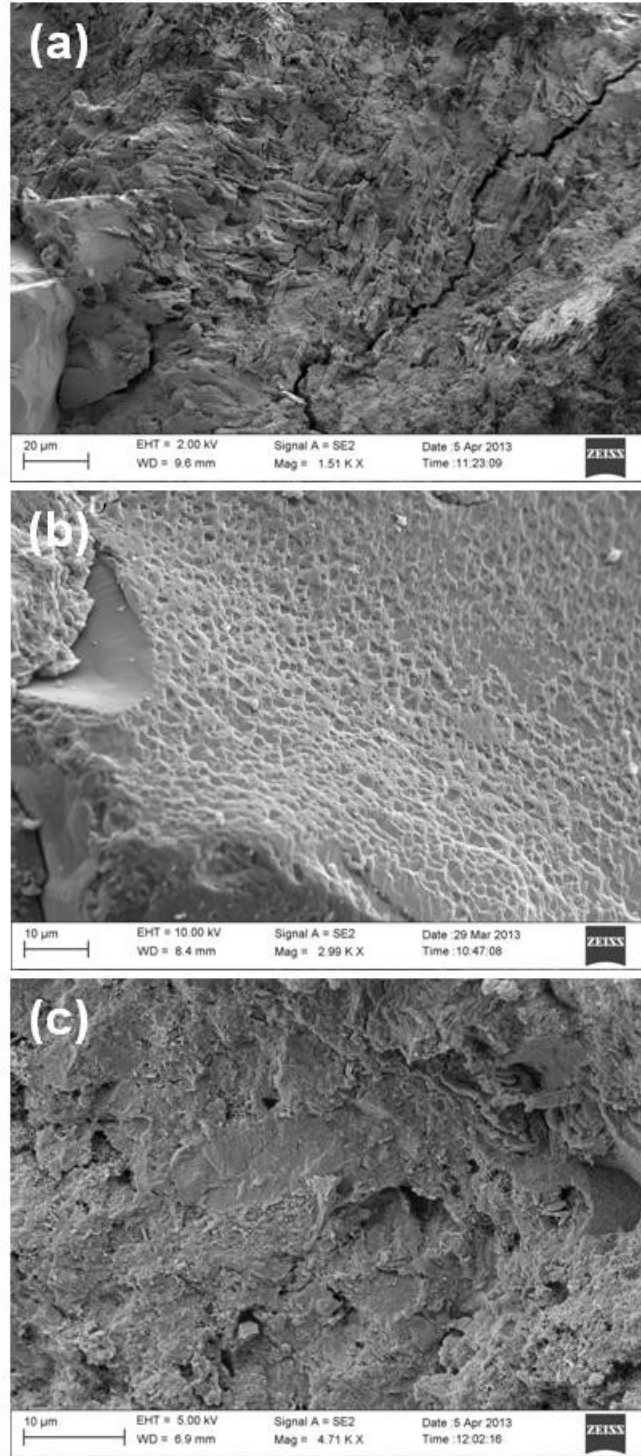


Figure 3. 5: Scanning electron micrographs of (a) control, (b) biopolymer added concrete at 7 days, and (c) biopolymer added concrete at 28 days.

BIBLIOGRAPHY

FHWA – Post Tensioning Tendon Installation And Grouting Manual, 2004

Durability And Sustainability of Concrete Bridges, PCI Presentation, 2009

Podolny, Walter Jr., 1992, "Corrosion of prestressing steels and its mitigation", PCI Journal, Volume: 37, Issue: 5.

Woodward, R.J. and William, F.W., 1988, "Collapse of Ynys – y – Gwas Bridge, West Glamorgan," Proceedings of Institute of Civil Engineers, Part 1, Volume.84, pp.635-669.

Florida Department of Transportation, 2001a, "Mid bay Bridge Post – Tensioning Evaluation," Final Report, Corven Engineering, Inc., FDOT, Tallahassee, FL, 2622pp.

Florida Department of Transportation, 2001b, "Sunshine Skyway Bridge Post – Tensioned tendons Investigation," Parsons Brinckerhoff Quade and Douglas, Inc., FDOT, Tallahassee, FL.

Electrochemical Characterization and Time Variant Structural Reliability Assessment of Post – Tensioned Segmental Concrete Bridges, Dissertation, Radhakrishna.G. Pillai, 2009.

Evaluation of External Post Tensioned Tendons Using Vibration Signatures, Dissertation, Jun Ki Lee, 2007

Dickson. T.J., Tabatabai. H., Whiting. D.A., "Corrosion Assesment of a 34 Year Old Precast Post – tensioned Concrete Girder", PCI Journal, Nov – Dec 1993.

Federal Highway Administration (FHWA), 2011, "Elevated Chloride Levels in Sika Grout 300 PT Cementitious Grout", Memorandum.

Li, Z., Zudnek, A., Landis, E., Shah, S., 1998, "Application of Acoustic Emission Technique to Detection of Reinforcing Steel Corrosion in Concrete," ACI Materials Journal, 95(1),68 – 76.

Ziehl, P., 2008, "Application of Acoustic Emission Evaluation for Civil Infrastructure," SPIE Smart Structures and Materials and Nondestructive Evaluation and Health Monitoring, San Diego, CA, 9 pp., March 9 – 13.

Mangual, J., ElBatanouny, M. K., Ziehl, P., and Matta, F. (2013). "Acoustic-Emission-Based Characterization of Corrosion Damage in Cracked Concrete with Prestressing Strand". ACI Materials Journal, 110(1), 89.

Mangual, J., ElBatanouny, M.K., Ziehl, P., and Matta, F. (2012). "Corrosion Damage Quantification of Prestressing Strands Using Acoustic Emission." ASCE Journal of Materials in Civil Engineering, in press.

Assouli B, Simescu F, Debicki G and Idrissi H. Detection and identification of concrete cracking during corrosion of reinforced concrete by acoustic emission coupled to the electrochemical techniques. *NDT & E International*. 2005; 38: 682-9.

Yuyama S, Yokoyama K, Niitani K, Ohtsu M and Uomoto T. Detection and evaluation of failures in high-strength tendon of prestressed concrete bridges by acoustic emission. *Construction and Building Materials*. 2007; 21: 491-500.

Ohno K and Ohtsu M. Crack classification in concrete based on acoustic emission. *Construction and Building Materials*. 2010; 24: 2339-46.

Kawasaki Y, Tomoda Y and Ohtsu M. AE monitoring of corrosion process in cyclic wet-dry test. *Construction and Building Materials*. 2010; 24: 2353-7.

Lyons R, Ing M and Austin S. Influence of diurnal and seasonal temperature variations on the detection of corrosion in reinforced concrete by acoustic emission. *Corrosion Science*. 2005; 47: 413-33.

Cullington DW, MacNeil D, Paulson P and Elliott J. Continuous acoustic monitoring of grouted post-tensioned concrete bridges. *NDT & E International*. 2001; 34: 95-105.

Perrin M, Gaillet L, Tessier C and Idrissi H. Hydrogen embrittlement of prestressing cables. *Corrosion Science*. 2010; 52: 1915-26.

Idrissi H and Limam A. Study and characterization by acoustic emission and electrochemical measurements of concrete deterioration caused by reinforcement steel corrosion. *NDT & E International*. 2003; 36: 563-9.

Ohtsu M and Tomoda Y. Phenomenological model of corrosion on process in reinforced concrete identified by acoustic emission. *ACI Mater J*. 2008; 105: 194-9.

Ramadan S, Gaillet L, Tessier C and Idrissi H. Detection of stress corrosion cracking of high-strength steel used in prestressed concrete structures by acoustic emission technique. *Applied Surface Science*. 2008; 254: 2255-61.

Feng X, Tang Y and Zuo Y. Influence of stress on passive behavior of steel bars in concrete pore solution. *Corrosion Science*. 2011; 53: 1304-11.

Broomfield, John P., “Corrosion of Steel in Concrete”, Second Edition, 2007.

Song, G., Shayan, A., “Corrosion of Steel in Concrete – State of the art Review”, ARRB Transportation Research, Review Report 4, July 1998.

Nair A and Cai CS. Acoustic emission monitoring of bridges: Review and case studies. *Engineering Structures*. 2010; 32: 1704-14.

Xu, J. (2008). “Nondestructive evaluation of prestressed concrete structures by means of acoustic emission monitoring”, Dissertation, Dept. of Civil Engineering, Univ. of Auburn, Auburn, Alabama.

Prestressed Concrete, Edward Nawy, Fifth Edition

Evaluation of External Post Tensioned Tendons Using Vibration Signatures, Dissertation, Jun Ki Lee, 2007

Hamilton. H.R., Wheat. H.G., Breen. J.E., Frank. K.H., “Corrosion testing of Grout for Post-tensioning Ducts and Stay Cables”, Journal of Structural Engineering, Feb 2000.

West. J.S., Breen. J.E., Vignos. R.P., “Evaluation of Corrosion Protection for Internal Prestressing Tendons in Precast segmental bridges”, PCI Journal.

Salas. R.M., Schokker. A.J, West. J.S., Breen. J.E., Kreger. M.E., “Corrosion Risk of Bonded Post Tensioned Concrete Elements”, PCI Journal, Jan – Feb 2008.

ASTM E1316 – 04, 2004,” Standard Terminology for Nondestructive Evaluation’, American Standard for Testing and Materials, (2000, Reapproved 2004).

Pellegrino C, Porto Fd and Modena C. Rehabilitation of reinforced concrete axially loaded elements with polymer-modified Cementitious mortar. *Construction and Building Materials*. 2009; 23: 3129-37.

Martinola G, Meda A, Plizzari GA and Rinaldi Z. Strengthening and repair of RC beams with fiber reinforced concrete. *Cement and Concrete Composites*. 2010; 32: 731-9.

Raupach M. Patch repairs on reinforced concrete structures – Model investigations on the required size and practical consequences. *Cement and Concrete Composites*. 2006; 28: 679-84.

Sharif A, Rahman MK, Al-Gahtani AS and Hameeduddin M. Behaviour of patch repair of axially loaded reinforced concrete beams. *Cement and Concrete Composites*. 2006; 28: 734-41.

Qiao F, Chau CK and Li Z. Property evaluation of magnesium phosphate cement mortar as patch repair material. *Construction and Building Materials*. 2010; 24: 695-700.

Pacheco-Torgal F, Abdollahnejad Z, Miraldo S, Baklouti S and Ding Y. An overview on the potential of geopolymers for concrete infrastructure rehabilitation. *Construction and Building Materials*. 2012; 36: 1053-8.

Mechtcherine V. Novel cement-based composites for the strengthening and repair of concrete structures. *Construction and Building Materials*. 2013; 41: 365-73.

Ohama Y. Recent progress in concrete-polymer composites. *Advanced Cement Based Materials*. 1997; 5: 31-40.

Ohama Y. Polymer-based admixtures. *Cement and Concrete Composites*. 1998; 20: 189-212.

Fowler DW. Polymers in concrete: a vision for the 21st century. *Cement and Concrete Composites*. 1999; 21: 449-52.

Gorninski JP, Dal Molin DC and Kazmierczak CS. Study of the modulus of elasticity of polymer concrete compounds and comparative assessment of polymer concrete and portland cement concrete. *Cement and Concrete Research*. 2004; 34: 2091-5.

Aggarwal LK, Thapliyal PC and Karade SR. Properties of polymer-modified mortars using epoxy and acrylic emulsions. *Construction and Building Materials*. 2007; 21: 379-83.

Decter MH. Durable concrete repair — Importance of compatibility and low shrinkage. *Construction and Building Materials*. 1997; 11: 267-73.